UNDERSTANDING THE LINK BETWEEN METEOROLOGY AND SPECIATED ABUNDANCE OF BIOAEROSOLS IN AN URBAN ENVIRONMENT

A Thesis
Presented to
The Academic Faculty

By

Arnaldo Negron Marty

In Partial Fulfillment
Of the Requirements for the Degree
Master of Science in the
School of Chemical and Biomolecular Engineering

Georgia Institute of Technology

May 2016

Understanding the Link between Meteorology and Speciated Abundance of Bioaerosols in an Urban Environment

Approved by:

Dr. Athanasios Nenes
School of Chemical and Biomolecular Engineering
Georgia Institute of Technology

Dr. Kostas T. Konstantinidis
School of Civil and Environmental Engineering
Georgia Institute of Technology

Dr. Mark P. Styczynski
School of Chemical and Biomolecular Engineering
Georgia Institute of Technology

Date Approved: March 16, 2016

DEDICATION

I dedicate this thesis to my beloved mother, Mayra Marty Mercado. She has been my support and motivation during this long journey. Since I was a child, believed in me and raised me with hunger for knowledge. She taught me knowledge is the only thing no one can steal from you and will remain with you until death. Furthermore, she inculcated great moral standards and values on me, which have been key elements to achieve my professional and personal goals. Thanks mother for been a great tutor and for all you sacrificed to help me become a professional and a good human being.

ACKNOWLEDGEMENTS

I would like to acknowledge the support of my group mates in Nenes Lab, especially to my advisor Dr. Athanasios Nenes for his unconditional support and advice during this journey. As well, want to thank Kostas Lab for their help and support in my biology training during these years. Last, but not least, I want to thank Dr. Natasha DeLeon Rodriguez for her dedication to train me in the bioaerosol lab techniques.

TABLE OF CONTENTS

LIST OF TABLES

LIST OF FIGURES

LIST OF SYMBOLS AND ABBREVIATIONS

C_{air}	Atmospheric Sample Air Basis Concentration
CCN	Cloud Condensation Nuclei
C_{liq}	Atmospheric Sample Liquid Basis Concentration
CP	Cleaning Protocol
CV	Coefficient of Variability
dN/dD_p	Frequency of Particle Size
DNA	Deoxyribonucleic Acid
EPM	Epifluorescence Microscopy
FBAP	Fluorescent Biological Atmospheric Particles
FCM	Flow Cytometry
FISH	Fluorescent in Situ Hybridization
FL1&3	WIBS Fluorescence Detector 1 and 3 Combination
FSC	Forward Side Scattering
FT	Force Trigger
HNA	High Nucleic Acid
I	Subpopulation Geometric Mean FSC-A Intensity
ID	Inner Diameter
IN	Ice Nuclei
LIF	Light Induced Fluorescence
LNA	Low Nucleic Acid

LPM	Liters per Minute
NADH	Nicotidanide Adenine Dinucleotide
N_{all}	WIBS Total Particle Concentration
OD	Outer Diameter
PBAP	Primary Biological Atmospheric Particles
PBS	Phosphate-buffered Saline
PMTs	Photomultiplier Tubes
PSL	Polystyrene Latex
qPCR	Quantitative Polymerase Chain Reaction
RH	Relative Humidity
RH_{ave}	Average Relative Humidity During SpinCon II Sampling Time
RNA	Ribonucleic Acid
S	Subpopulation Mean Size
SD	Standard Deviation
SEM	Scanning Electron Microscope
SSC	90^0 Side Scattering
T_{ave}	Average Temperature During SpinCon II Sampling Time
TBAP	Total Biological Atmospheric Particles
TFE	Thermally Assisted Field Emission
UV-APS	Ultraviolet Aerodynamic Particle Sizer
WIBS	Waveband Integrated Bioaerosol Sensors

CHAPTER 1

INTRODUCTION

Over the years bioaerosols have been of substantial interest given their possible importance to cloud formation, pulmonary diseases, and detection and quantification of bioterrorism attempts. Biological particles may influence climate and the hydrological cycle by serving as cloud condensation nuclei (CCN) and ice nuclei (IN) in cloud formation (Morris et al., 2014; Möhler et al., 2007). The interaction of biological particles with the atmosphere is of substantial importance to us given its direct effect on our way of living. Morris et al., 2014 proposed a possible bioprecipitation cycle by which plants may generate small nucleator bioparticles that could be integrated in clouds and play an important role in precipitation formation. A change in precipitation zones caused by global warming may change the communities and abundance of biological particles in certain ecosystems, which will affect microbe dispersal and our susceptibility to allergies and pulmonary diseases. DeLeon-Rodriguez et al., 2013 indicated airborne microbial cells may be more important to cloud formation than previously suggested given the substantial bacteria concentrations quantified in the mid to upper-troposphere. They also emphasized the importance of improving techniques to identify and quantify airborne cells and of understanding better their impact on precipitation.

Microbe detection and quantification have been challenging due to the low concentrations and cultivability found in the atmosphere. A small fraction of the atmospheric microorganisms can be cultured, which is one of the reasons why cultivable methods had underestimated the abundance and viability of bioaerosols by up to two

orders of magnitude (Chi and Li et al., 2007). Since researchers proved non-cultivable methods are more effective, Epifluorescence microscopy (EPM) has become the standard for bioaerosol quantification. However, this technique is quite time consuming, relies on the researcher's judgment and is subject to large uncertainties. Other non-cultivable molecular biology quantification techniques have been applied like fluorescent in situ hybridization (FISH), flow cytometry (FCM), and quantitative polymerase chain reaction (qPCR) in order to learn more about their relative abundance, cell cycle and viability. FCM has proved to be as reliable as EPM, showing lower uncertainty and higher quantification and taking less time than EPM (Lange et al., 1997). Also, FCM possesses certain advantages including (i) the ability to produce multi-parameter analysis, (ii) the generation of single cell information and (iii) the capability of high sample processing rates, which make it a useful technique not just to quantify microbes, but to understand their lifecycle.

The primary biological atmospheric particles (PBAP) consist of a diverse group of bioparticulate emitted from the biosphere to the atmosphere, which can be whole organisms (e.g bacteria, diatoms, algae), reproductive cells (e.g. pollen, fungal spores, mosses), biopolymers (e.g. DNA, chitin and cellulose), plant and insect debris. Among all different types of PBAP, bacteria, fungal spores and pollen dominate the concentration of atmospheric bioparticles. PBAP concentrations in urban areas have been estimated to be 10^4 to 10^6 part. /m^3. Bacteria (10^3- 10^6part. /m^3), fungal spore (10^3 – 10^5 part. /m^3) and pollen (10 - 10^3 part. /m^3) atmospheric concentrations have been estimated in the same manner (Bowers et al., 2011; Chi and Li, 2007; Bauer et al., 2008; Liang et al., 2013; Silijamo et al., 2008). As well, previous literature suggests that PBAP can make up to

30% of fine and 70% of coarse particulate matter (PM) in rural and rain forest atmospheres (Pöhlker et al., 2012; Jaenicke, 2005; Elbert et al., 2007). Among PBAP, fungal spores account for a large portion and represent around 50 Tg yr^{-1} of the global emission, which is comparable to the emission of anthropogenic primary organic aerosols (Elbert et al., 2007). However, uncertainty remains in their quantification, and it is still a challenge to understand the diurnal and meteorological variability of their abundance and composition.

FCM is a single-cell analysis to study cell lifecycle by measuring light scattering and fluorescence intensity (*Wang; et al 2010)*. It is a common technique used in immunology and biomedical research to count and understand the eukaryotic cell lifecycle. It has also been used in microbiology to quantify pure cultures of yeast and different types of bacteria (Nir et al., 1990; Van Dilla et al., 1983). It consists of a technique in which particles suspended in liquid solution flow through an interrogation point. Particles in the sample flow are hydrodynamically focused by a faster sheath flow, which will ensure the flow of one particle at a time through the detection point. Then particles are triggered by a laser beam, and the resultant light scattering and fluorescent emissions are measured by their respective detectors. Forward side scattering (FSC), light scattering parallel to the laser beam, is measured by the FSC photodiode. Side scattering (SSC), 90º light scattering, is measured by the SSC photodiode as is shown in Figure 1. Fluorescence is measured in specific wavelengths related to the fluorescent molecules present in the particles. Photons of light falling upon the detectors are converted into an electrical impulse by the photomultiplier tubes (PMTs) based on the area or the height of the recorded pulse. This impulse is then translated to a numeric signal by an AD (analog-to-

digital) converter. Biological particles are specifically detected by labelling with fluorescent molecules, which emit fluorescence when they bind to specific molecules in the microorganism. Several probes have been used for staining environmental DNA like: DAPI (4', 6-Diamidino-2-phenylindole), SYBR green, SYTO-13 and acridine orange (AO). Among them, SYTO-13 has been effective to quantify planktonic bacteria in aquatic systems. SYTO-13 is a cyanine nucleic acid stain, which binds to the nucleic acids present in the RNA and DNA of the cells. Its DNA and RNA emission/excitation wavebands are 488/509 nm and 491/514 nm, respectively. Previously, FCM has been used in immunology, biomedical and microbiology fields successfully. Aquatic environmental samples have also been successfully analyzed to differentiate between low nucleic acid (LNA) and high nucleic acid (HNA) phytoplankton and understand their lifecycle *(*Wang Y. et al 2010; Müller et al., 2010*)*. Chen and Li, 2005 applied FCM to atmospheric samples, but could not identify well-defined subpopulations of PBAP. In the same study Chen and Li, 2005 determined SYTO-13 to be the most effective nucleic acid stain to determine the total concentration of bioaerosols among the five different nucleic acid stains used. Additionally, FCM has been applied to atmospheric samples stained with Calcofluor-White-M2R to quantify fungal spore populations during spring in China. Results show a linear correlation between fungal spore concentrations and arabitol and mannitol concentrations (Liang et al., 2013). However, the identified populations are not well defined, and it is not clear the specificity of the technique toward each type of bioaerosol.

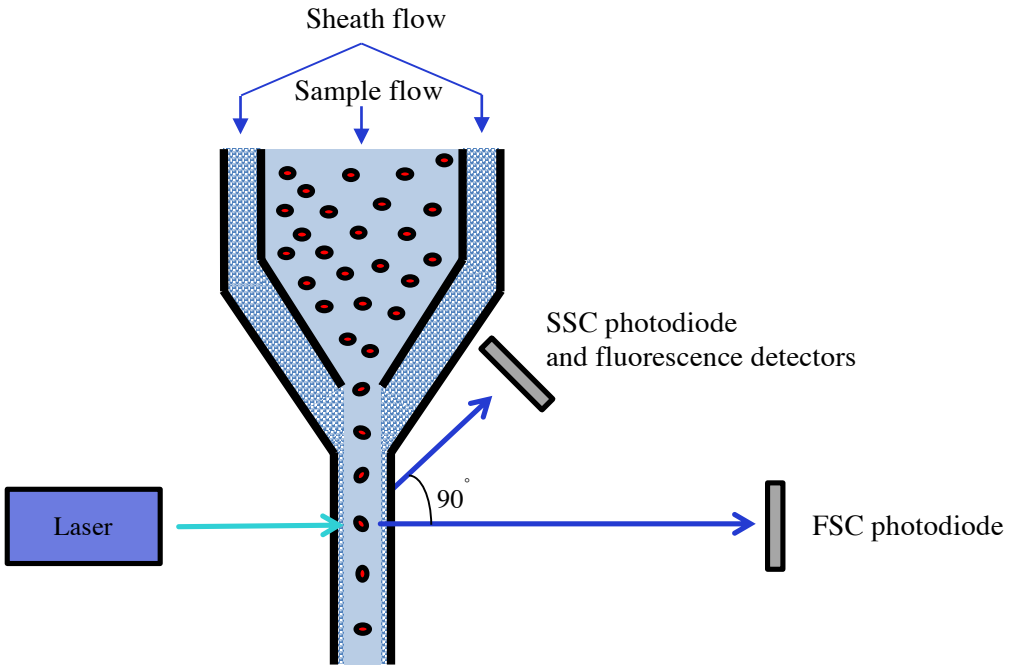

Figure 1: General diagram of flow cytometry optics and microfluidics

The Light Induced Fluorescence (LIF) technique has been increasingly used for bioaerosol quantification by measuring the autofluorescence intensity of specific high yield fluorophores present in PBAP. It relies on the basic assumption that the intrinsic fluorescence of biological material exceeds that of the potential interfering non-biological matter. PBAP fluorescence peaks have been related to Nicotinamide Adenine Dinucleotide (NADH) co-enzyme, flavins and amino acids like Tryptophan and Tyrosine in microorganisms. Their difference in fluorescence intensity with respect to non-biological particles has helped to distinguish PBAP and non-PBAP and to quantify in real-time the amount of fluorescent biological atmospheric particles (FBAP). This technique has enabled real-time measurements without the use of consumables. Several instruments have been used for FBAP detections, including UV-APS, WIBS-3, and WIBS-4. Together have led to better understanding of biological particle abundance and

diurnal cycles in different ecosystems. In forests, researchers seen FBAP diurnal cycles with a maximum concentration during evening and a minimum around mid-day. This behavior has been related to the temperature and relative humidity release mechanism of certain fungal spore species (Gabey et al., 2010; Tropak and Schnaiter., 2013; Wu et al., 2007). As a result, it is understood that fungal spores dominate the total FBAP in highly vegetative environments. However, urban areas have shown lower abundance of FBAP and different diurnal cycles and size distributions given the high diversity of PBAP and non-PBAP aerosols present in cities. Huffman et al., 2010 used the UV-APS to show a strong 3 μm-particle diurnal cycle in a Mainz, Germany semi-rural area between August and November, with a maximum in the mid-morning after sunrise and a constant background throughout the rest of the day. Gabey et al., 2011 used WIBS-3 to show two mid-morning concentration peak of 1.2 μm and 3.0 μm particles. The 1.2 μm peak seems to be related to the non-fluorescent particles, which means combustion product particles cannot be discarded as a possible source of fluorescent particles. Tropak and Schnaiter., 2013 showed by laboratory experiments that mineral dust, soot, and ammonium sulfate may be misclassified as biological particles when the total FBAP concentration is determined. In addition, we must be aware of the influence of combustion products and anthropogenic aerosols emitted in the studied environment. Urban areas could have different PBAP behavior influenced by regional factors and the surrounding ecosystems. Recently, Hernandez et al., 2016 have studied bacteria (n = 15), fungal spores (n = 29), and pollen (n = 13) species by characterizing their optical size, fluorescence type frequency, and fluorescence intensity. They concluded that WIBS-4 FL1 detector might more frequently detect bacteria and fungal spores. However, pollen showed higher

frequency to the combination of all detectors. In general, the study is the first step to create a catalogue of atmospheric sample observations, which help to decide the most effective type of fluorescence for PBAP quantification. LIF technique has biases to detect atmospheric biological particles as any other technique could have, but has been very effective for real-time measurements. As result, lab and field experiments must be combined to develop a better understanding of the complex microbial communities in the atmosphere.

Atlanta is a highly populated city surrounded by vast vegetative areas. Its weather is particularly humid and warm during spring and summer, which makes it an ideal location for bioaerosols research. Atmospheric biological particles collected in liquid solution have been difficult to quantify due to the low effectiveness of the impingement samplers to concentrate bioparticles to a detectable and robust amount. This study is the first to develop a FCM protocol to identify and quantify well-defined, speciated bioaerosols populations from samples collected with the SpinCon II. The FCM protocol includes cleaning protocols to minimize and constrain particle accumulation in the collector for a reliable quantification. Several samples were collected during spring 2015 to understand better bioparticle populations in Atlanta under different meteorological conditions, which then were compared to WIBS-4 data collected at the same time. The aims of the study were: (i) to develop an effective and reliable FCM detection and quantification protocol; (ii) to apply the protocol to understand bioparticle subpopulations and their variability in Atlanta area during different meteorological conditions; and (iii) to compare FCM and WIBS-4 results to have a better understanding of PBAP day-to-day variability.

CHAPTER 2

INSTRUMENTATION AND METHODOLOGY

2.1 Location of Sampling Site

Experiments were conducted at the rooftop-sampling platform of the ES&T building at Georgia Tech in Atlanta (33°46'44.5"N, 84°23'45.6"W) from March to September 2015. Multiple forest areas and possible bioaerosol sources surround the city placed in the southeastern USA, like: the Oconee National Forest to the southeast, Chattahoochee National Forest to the north, and Talladega National Forest to the west. WIBS-4, placed inside the building, sampled outside using ¼OD conductive tubing and the inlet was fixed 9 ft. above the sampling platform floor. It ran continuously during the April to May period. SpinCon II was placed in the platform during sampling episodes with its inlet pointing south. Fifteen Spincon II samples were collected during the April to May sampling events. Additionally, we collected three samples during rainy episodes from September 9, 2015 to September 11, 2015.

2.2 Sampler and Sample Collection

Sampling was performed using SpinCon II (InnovaPrep LLC, Inc.), a wet walled cyclone portable air sampler, which concentrates atmospheric aerosol in a liquid solution and uses a fluid level sensor to maintain sample volume constant during the sampling cycle. Figure 2 shows the design of the state-of-the-art sampler and its main parts. Figure 3a shows the instrument setup and Figure 3b shows a close-up of the sampler. It consists mainly of a blower pulling atmospheric particles by a slot inlet to a wetted wall

concentrator/collector where particles are suspended in PBS/Milli-Q water solution. The sampler is connected to a programmed control box where the sampling time, blower power supply, and fluid supply to extraction pumps can be controlled. SpinCon sampling is an inertia driven collection by which small particles (1-15 μm) stay in solution, but bigger particles deviate from the flow streamlines and deposit on the walls.

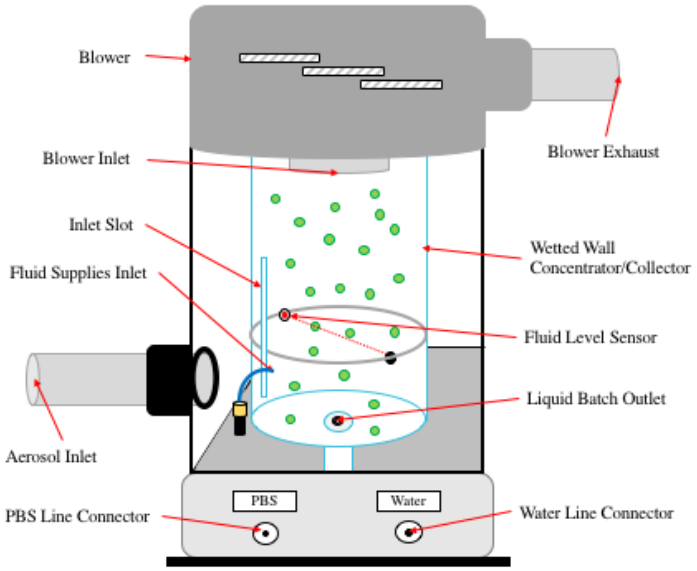

Figure 2: SpinCon II parts and design diagram.

Samples were collected on March 2015 during the design of the protocol. Then, three consecutive samples per week were collected from April 7th to May 15nd between 11am and 5pm Atlanta local time. SpinCon sampling efficiency was 39% in the 1 to 5 μm particle range. Even with a lower efficiency than impingement samplers, the SpinCon has better performance - product of the flow rate and the sampling efficiency - due to its high volumetric flow rate, which makes it more suitable for bioaerosol detection (Kesavan et al., 2015). Kesavan et al., 2015 analyzed the efficiency, power consumption,

and performance of 29 biosamplers to determine which of them could be best to use in an indoor or outdoor environment. They concluded that a biosampler's effectiveness will be determined by their performance in the size range of interest, rather than just by looking at its overall sampling efficiency. Our instrument was run at 478 L/min for 4 hr sampling cycles. Phosphate-buffered saline (PBS) 1X pH 7.2 solution was used and the instrument compensated evaporation by supplying Milli-Q water to maintain PBS concentration constant. It was programmed to dispense the sample in a 15 mL centrifuge tube after the sampling cycle finished. Then 10 μL of 37 wt. % formalin per mL of solution was added to every sample for preservation and samples were stored in a 4°C fridge. The instrument was modified and a cleaning protocol (CP) has been developed, as described below.

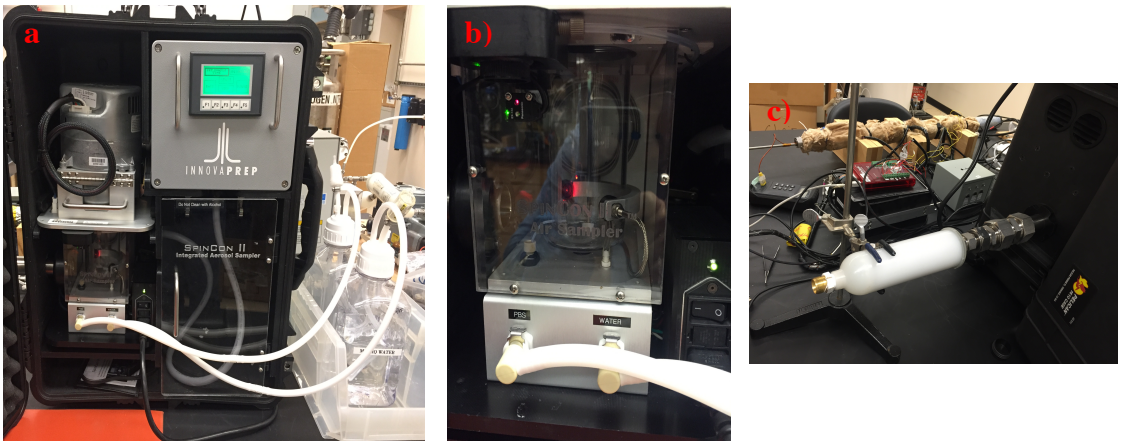

Figure 3: SpinCon II pictures, a) shows the instrument with its new fluid bottles system, b) shows a zoom in of the particles collection/concentration area and c) shows the HEPA filter connection in the SpinCon II inlet during the cleaning protocol.

2.3 SpinCon II Modifications

SpinCon II H_2O and PBS IV bags supplies were replaced by two-liter autoclavable Nalgene bottles (Thermo Scientific Inc.) with antimicrobial tubing and connectors. Also, a small HEPA filter was connected to prevent coarse and submicron

particles contamination; as illustrated in Figure 4. Two-liter Nalgene bottles were used to place all the sterilized fluids (Milli-Q water, PBS, 10 wt.% bleach solution and 70wt.% ethanol solution) involved in the cleaning and operation of the SpinCon II. Before every bottle of fluid was prepared, the connection lines and a small HEPA filter connection were cleaned with ethanol 70 wt.%. Once the connections were dried, fluids were transferred and the bottles were closed. Bottles were not opened again until the fluids were exhausted to ensure sterility. The connection to the SpinCon II consisted of a ¼'' Hose Barb elbow connected to the antimicrobial tubing and ultimately the two-liter Nalgene bottle. Fluids were sterilized with a 0.2 μm pore bottle top filters (Thermo Fisher Inc.) and transferred inside a biosafety cabinet. Then an aliquot of each fluid was collected after preparation to check sterility by epifluorescence microscopy and FCM.

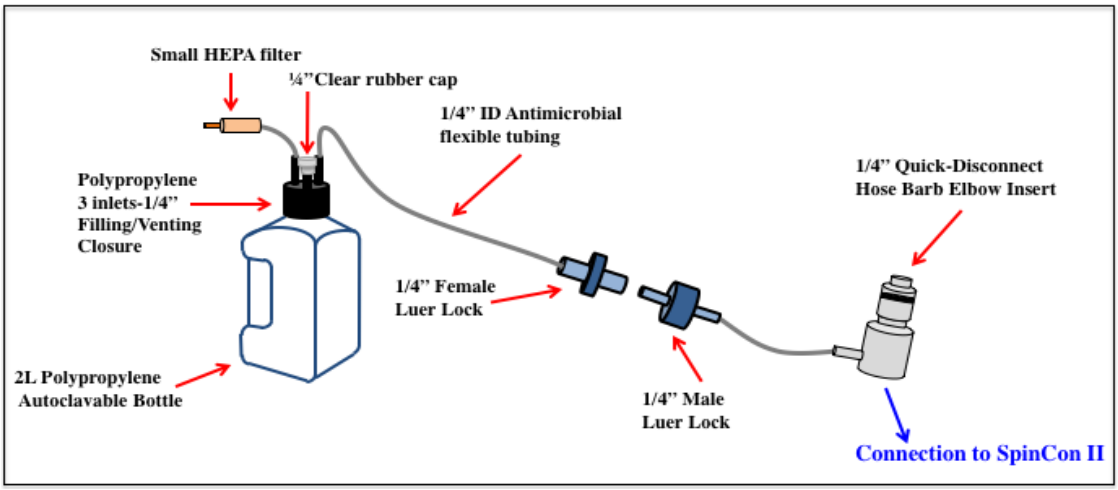

Figure 4: New fluids supply Nalgene bottle system design

2.4 Volumetric Flow Rate Measurements

SpinCon II volumetric flow rate was measured with a VT100 Hotwire Thermo-anemometer (Cole Palmer Inc.) using a 3 hole round duct transverse approach, shown in Figure 5. A 1 ¼'' OD tube with the same diameter as the SpinCon II inlet was designed

with 3 holes 60° apart traversing the tube axial flow direction. Triplicated velocity measurements were taken in the center of the tube (green dot in Figure 5) and the volumetric flow rate was calculated using the following equation:

$$Volumetric\ flow\ rate = \left(\frac{\pi}{4}\right) * (ID)^2 * air\ flow\ velocity \quad [1]$$

where ID is the inner diameter of the tube and the air flow velocity is the speed of flow measured by the anemometer. The average volumetric flow rate was 478 ± 6 L/min, which represents a 6% difference to the 450 L/min flow rate reported by InnovaPrep Inc. The flow was considered turbulent with radial air velocity assumed constant.

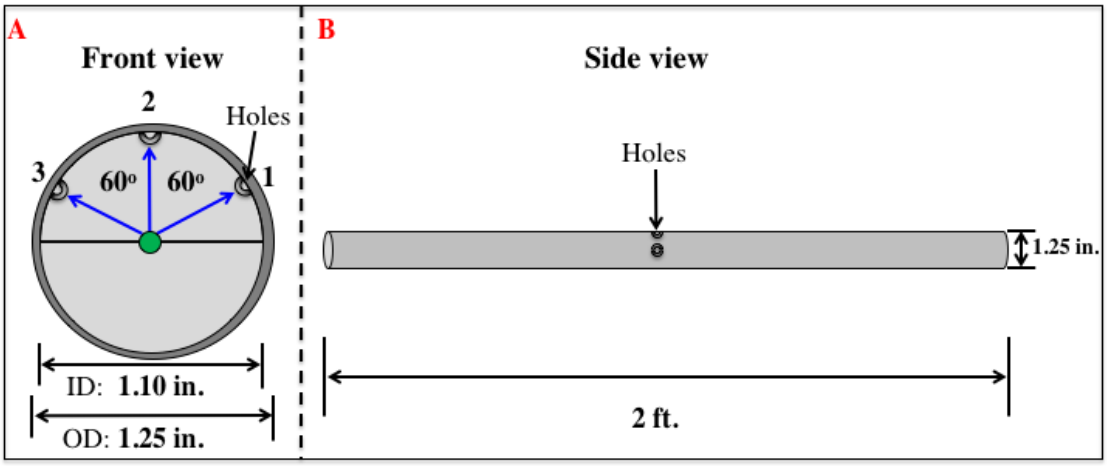

Figure 5: Tube design used to perform volumetric flow rate measurements of the SpinCon II; a) shows the front view of the tube with the description of the holes where measurements were taken with the hotwire anemometer, and b) shows the side view of the tube.

2.5 Cleaning Protocol (CP)

The cleaning protocol consisted of two phases. During phase one, the interior and exterior of the instrument were cleaned. The front acrylic window was removed to clean all acrylic windows and the outside of the collector/concentrator with ethanol 70 wt.%. Then the instrument inlet and outlet were cleaned and the inside of the collector

/concentrator was cleaned with ethanol 70 wt.%. During the second phase, the SpinCon II inlet was connected to a HEPA filter to avoid particles entering the system (as shown in Figure 3c). Then the instrument was washed with ethanol 70 wt.%, 10 wt.% bleach solution, 1X PBS, and Milli-Q H_2O in this order. The wash consisted of the following steps: a rinse, a 2-minute sample, and filling the instrument collector/concentrator with the fluid in use. The collector/concentrator was drained after 1 minute. The same steps were repeated for the remaining fluids. Then a blank was taken to constrain the residual particles after the CP. Finally, the HEPA filter was disconnected, instrument inlets and outlets were sealed and the inlet tube was cleaned with ethanol 70 wt.% to be ready for rooftop sampling. SpinCon II was rinsed with ethanol 70 wt.% after each sampling episode and the cleaning protocol was applied before sampling.

2.6 FCM Methodology

A flow cytometer is a single-cell analysis instrument used for particles in liquid solution. The technique uses light scattering and fluorescence intensity to differentiate particles (biotic or abiotic particles) by size and specific cell functional labelling, respectively. During the study, a BD Accurri C6 flow cytometer (BD Bioscience Inc.) was used without modifications to analyze samples collected with the Spincon II. The instrument is capable of quantifying cells due to its ability to control the sample flow rate by adjusting flow velocity in three modes (slow: 14 μL/min, medium: 35 μL/min, and fast: 66 μL/min). It possesses four fluorescence detectors: FL1 533/30 nm, FL2 585/40 nm, FL3 > 670 nm and FL4 675/25 nm, which make it possible to analyze the fluorescence emission of multiples probes. Accurri C6 pulls the sample to the interrogation point, instead of using pressurized flow to push it. Figure 6 illustrates the

general optics and fluidics diagram of the instrument. Moreover, it has the detectors organized in an octagon with fixed alignment, which makes its operation straightforward.

A 2.5 μM SYTO-13 nucleic acid probe was added to the fixed samples, which were incubated for 15 min at room temperature to stain biological particles. 10 μL of 15 μm polystyrene beads were added to the 1 mL volume samples for quantification. BD Accurri C6 was cleaned before use with 0.2 μm filtered Milli-Q water in fast mode for 10 min to minimize background noise to 1 part/μL. At the beginning of each experiment, a 1 mL blank of the atmospheric sample without SYTO-13 was analyzed, which will be used in quantification calculations. Each sample was run in slow mode for 5 min. Then, the instrument was cleaned with 0.2 μm filtered Milli-Q water in slow mode for 1 minute to eliminate any accumulation from the previous sample which is important due to low atmospheric particle concentrations. SYTO-13 fluorescence intensity was measured by FL1-A detector and used in combination with other parameters (e.g., FSC-A, SSC-A and FL4-A) to understand the data. A 80,000 FSC-H threshold was set in the instrument during data acquisition to remove non-fluorescent particles smaller than 1 μm and enable better visualization of biological populations. Results were analyzed with FlowJo software and contour plots were generated to gate and quantify bioparticles population (see Appendix A: Figure 26).

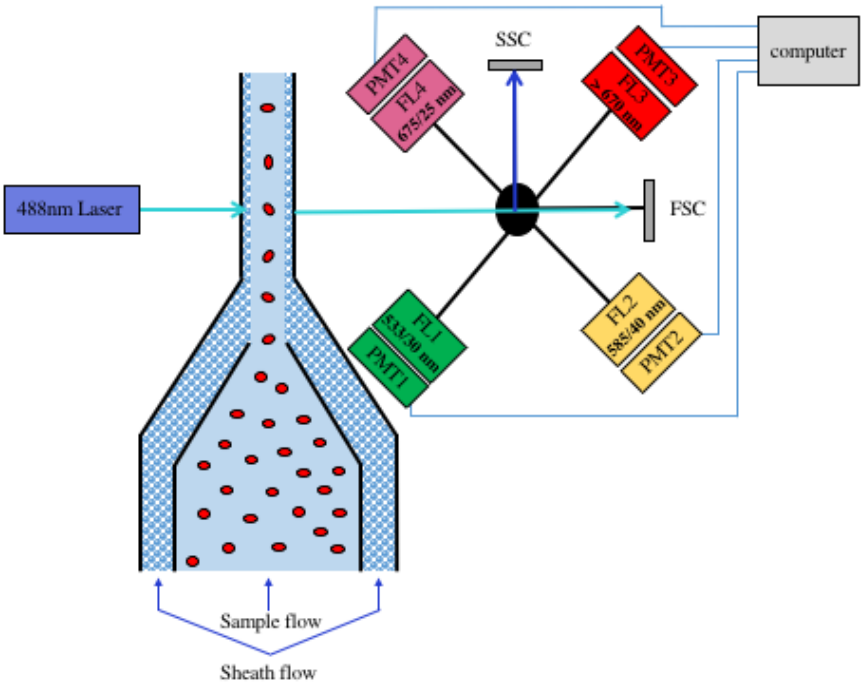

Figure 6: BD Accuri C6 flow cytometer optics and fluidics diagram.

2.7 Constraining Particle Accumulation by FCM

Several blanks were taken to ensure that the accumulation of particles, due to fluids and SpinCon II cleanliness, did not affect biological population identification and quantification. PBS and Milli-Q water blanks were analyzed by EPM and FCM. Microscopy results did not show any biological contamination. The FCM results confirmed that the fluids total biological particle concentration contribution is negligible to the total biological atmospheric particles (TBAP) concentration of the collected samples. Additionally, a 2-min blank was taken after the CP to constrain residual particles. The total accumulation of biological particles inside the instrument after the 4 hr sampling period was constrained by the HEPA filter blank, which consisted of running the instrument for the same time that the samples were collected on the rooftop with a HEPA filter connected to the inlet of the SpinCon II. Thereafter, a 4 hr atmospheric

sample collection showed that the accumulation of biological particles in the blank represented around 1% of the TBAP in the atmospheric sample.

2.8 FCM Calibration Beads Experiments

The mean size of each subpopulation was determined by comparing 1, 2, 4, 6, 10 and 15 μm standardized beads (Flow Cytometry calibration kit, Life Technology Inc.) FSC-A scattering distributions with the subpopulations FSC-A scattering distributions. First, standardized beads were analyzed in triplicate by FCM. Then the geometric mean FSC-A intensities were calculated for each beads size (using FlowJo). Two samples were prepared: a) having 10μL of 1, 4 and 10 μm beads; and b) having 10μL of 2, 6 and 15 μm beads; both were diluted to 1 mL with Milli-Q water. Samples SSC-A vs. FSC-A plots are shown in Figure 7.

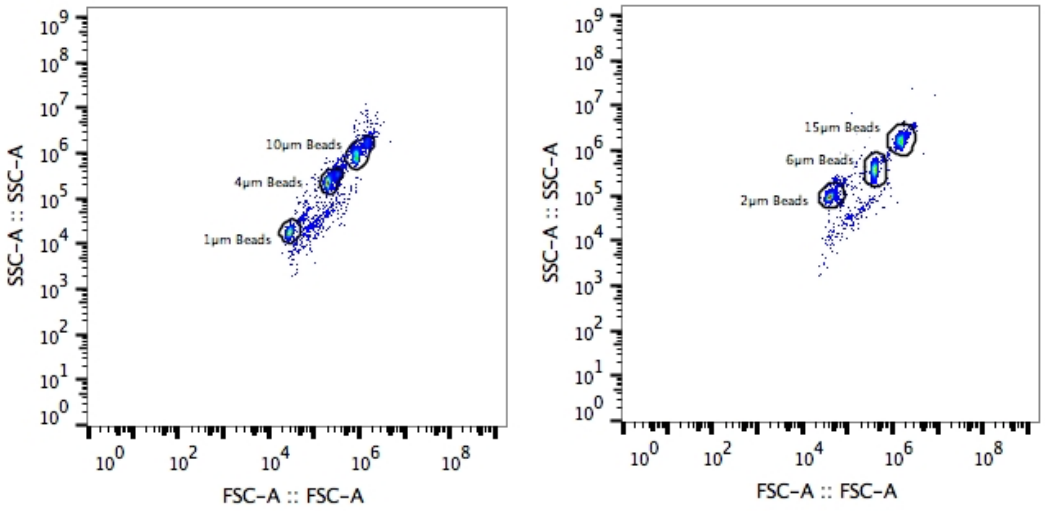

Figure 7:SSC-A vs. FSC-A plots of the FCM calibration beads experiments showing the different type of beads used for size calculations.

2.9 WIBS-4 (Waveband Integrated Bioaerosol Sensor Model 4)

WIBS-4 is a single biological particle real time sensor, which measures particle light scattering and autofluorescence in an approximately 0.5-16 μm particle range.

Particles are initially sized using the 90-degree side-scattering signal detected in fluorescence channel 2 from a 635 nm continuous-wave diode laser. The diagram shown in Figure 8 gives us a better description of the location of each light source, scattering and fluorescence detectors, and sample flow direction of WIBS-4. The scattering intensity is directly related to the particle diameters of NIST-traceable polystyrene latex spheres (PSLs with 0.8, 0.9, 1.0, 1.3, 2.0, 3.0 μm diameter, Thermo Scientific Inc.) used to calibrate the instrument prior to deployment. Thus all WIBS sizing is optically referenced to a PSL material refractive index of 1.59. Then a 280nm and 370nm pulsed xenon flashtube UV sources are used to measure the particles autofluorescence. Three important fluorescent emissions are measured: (i) FL1: excitation at 280nm and emission in 310-400nm, (ii) FL2: excitation at 280nm and emission in 420-650nm; and (iii) FL3: excitation at 370nm and emission in 420-650nm. FL1 emission has been related to Tryptophan, Tyrosine and Phenylalanine emission, highly fluorescent amino acids present in microorganisms cell wall (Pöhlker et al., 2012). FL2 and FL3 emissions have been related to Nicotinamide Adenine Dinucleotide (NADH) emission. Biological and non-biological particles can be discriminated by setting a fluorescent intensity threshold. We used Gabey et al., 2010 approach, but FL1 was considered to calculate the total FBAP concentration. FL1 has shown to be sensitive to ammonium sulfate and other non-biological particles (Tropak and Schnaiter, 2013), which may overestimate particles in 0.5 – 1.5 μm size range. As result, the total FBAP concentration based on FL1 channel was consider an overestimation of the total FBAP concentration. FL2 was not included in FBAP calculations due to its high cross-sensitivity to non-biological aerosols (Gabey et al. 2011). WIBS-4 collected data uninterrupted during the study and force trigger (FT)

calibrations were taken every 24 hr. Its total volumetric flow rate was adjusted to 2.3 LPM, which was splitted into a 0.3 LPM sample flow rate and a 2.0LPM sheath flow rate.

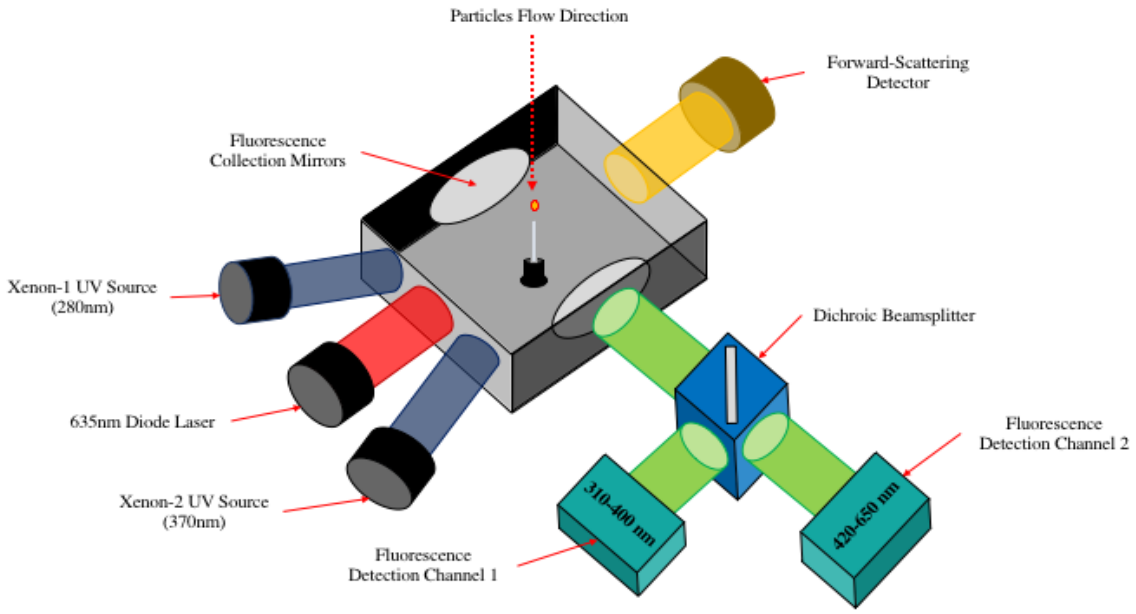

Figure 8: WIBS-4 optics and fluidics general diagram

2.10 Meteorological Data

Meteorological data was acquired from the ES&T building weather station at Georgia Tech. The data was analyzed in a 1 min resolution and the following meteorological variables were used within the study: wind speed, wind direction, relative humidity (RH), temperature, total hourly rain and UV radiation index. Temperature, RH, wind speed and wind direction were averaged during SpinCon II collection events to better understand the predominant meteorological conditions. As well, were used in WIBS-4 data analysis to understand FBAP variability under different meteorological scenarios.

2.11 SEM and EPM Pictures

1 mL of fixed atmospheric sample was filtered through a 0.2 μm Nucleopore filter for each sample to be analyzed by the Scanning Electron Microscope. The filters were attached to 25 mm mounters and coated with a gold/carbon sputter. Then, pictures were taken to samples collected on April 14, 2015 using a LEO 1530 Thermally-Assisted Field Emission (TFE) Scanning Electron Microscope (SEM). Also, Epifluorescence microscopy (EPM) pictures were taken during the design of the FCM protocol. Samples were stain using the Live/Dead staining kit. The 1 mL stained sample was incubated for 15 min; then was filtered in a 0.2 μm black Nucleopore filter and placed in a glass slide. Samples were observed in the Axion Observer D1 Epifluorescence Microscope (Zeiss).

2.12 FCM Pure Cultures Experiments

Pure culture experiments were performed during the study as an additional support to the observations seen in the atmospheric samples. Two different types of experiments were conducted: i) the individual microorganisms (bacteria, yeast and pollen) were analyzed to visualize the population of microorganisms; ii) mixtures of the microorganisms were analyzed to understand how they compare with what is seen in the atmospheric samples.

Yeast used in the experiments is the Y55 strain of *S. cerevisiae* and bacteria (F8) is a *Pseudomonas* atmospheric isolate strain. They were grown overnight in non-limited oxygen conditions. Y55 was grown in 1X yeast extract at 35°C and F8 was grown in 1X LB broth at 30°C. Then an aliquot of each was fixed with formalin. Ragweed pollen (*Ambrosia artemisiifolia*), purchased to Greer Laboratories (Lenoir, NC), was used without further purification. A 10 mg/mL pollen/PBS solution was prepared as working

stock. Different dilutions were performed to yeast, bacteria and pollen samples to reach 10^4 - 10^5 part. /mL concentration and were individually analyzed by FCM. Finally, mixtures of the microorganisms were analyzed using the same SYTO-13 and 15 μm beads concentrations used in the atmospheric samples.

CHAPTER 3

ROOFTOP SAMPLING RESULTS

3.1 Data Processing and Analysis

3.1.1 FCM Biopopulation Identification and Quantification

Rooftop samples showed a heterogeneous population of particles after FCM analysis. FL1-A vs. SSC-A and FL1-A vs. FSC-A plots were used to better understand the observed subpopulations. FL1-A detector measured SYTO-13 fluorescence intensity, FSC-A measured the forward scattering intensity related to the particle size and SSC-A measured the side scattering intensity related to the particle internal complexity or granularity. Different subpopulations were identified, as shown in Figure 9.

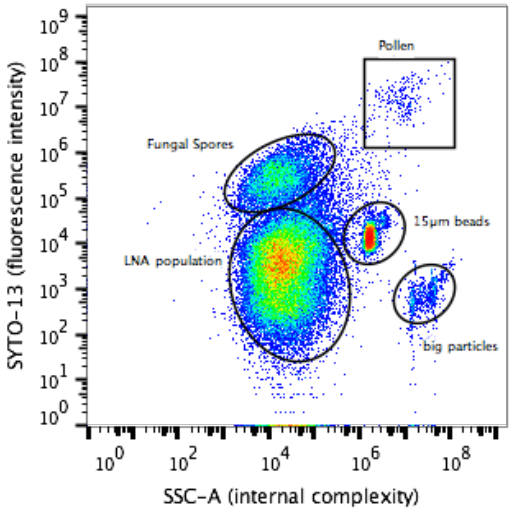

Figure 9: FL1-A vs. SSC-A plot used to identify subpopulations in collected rooftop atmospheric samples.

Among the heterogeneous population, five subpopulations were identified: low nucleic acid (LNA), fungal spores, pollen, 15 μm beads and big particles. Additional EPM and SEM pictures in Figures 10 and 11, taken during the design of the FCM protocol, show the presence of a heterogeneous population of biological particles. The 15

μm beads subpopulation was known to be present because were added as standards for quantification. Big particles were observed in several samples, but were not quantified due to their inconsistency and our focus on biological particles. Among them, we focused on the variation of the low nucleic acid (LNA) and high nucleic acid (HNA), which we called LNA and fungal spore subpopulations, respectively. Previously, LNA and HNA subpopulations have been identified in aquatic environment by using nucleic acid stains like: SYTO-13, SYBR green, and DAPI (Wang Y. et al., 2010; Bouvier, T. et al., 2007; Lebaron, P. et al., 2001). However, this study is the first to identify and quantify LNA and HNA subpopulations of atmospheric microorganisms; and to study their variability due to meteorological factors.

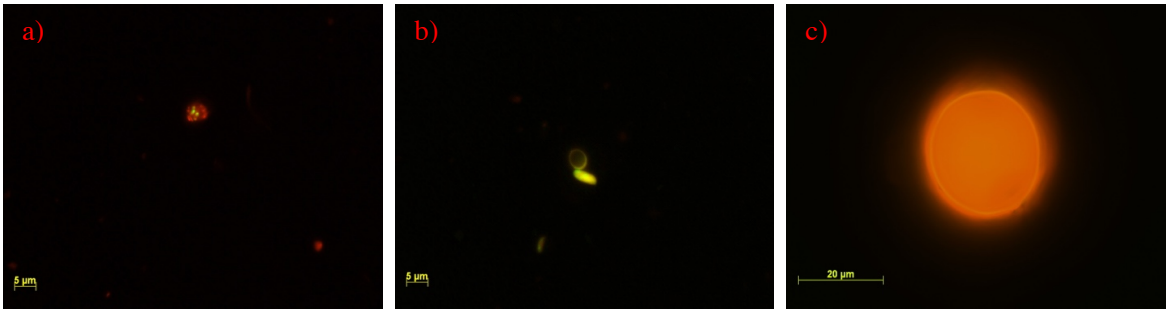

Figure 10:EPM pictures of atmospheric samples collected in March 24, 2015 showing different types of biological particles. a) shows a bacteria agglomerate, b) shows two attached fungal spores and c) shows ~20 μm pollen particle.

The HNA subpopulation, referred to as the fungal spore subpopulation hereafter, showed a dependence on relative humidity and 3-5μm mean size based on the FSC-A geometric mean intensity of the particles (look section 3.1.2). In addition, results show the HNA subpopulation was completely depleted during long dry episodes and well defined during high RH % episodes, especially after rain events (Look section 3.2.2 and section 3.2.3). Researchers linked this behavior to the release mechanism of different fungal spores like ascospores and basidiospores genus. They are aerosolized frequently

during humid and after rain events given its release mechanism dependence on temperature and relative humidity (Oliveira et al., 2000; Li and Kendrick, 1995).

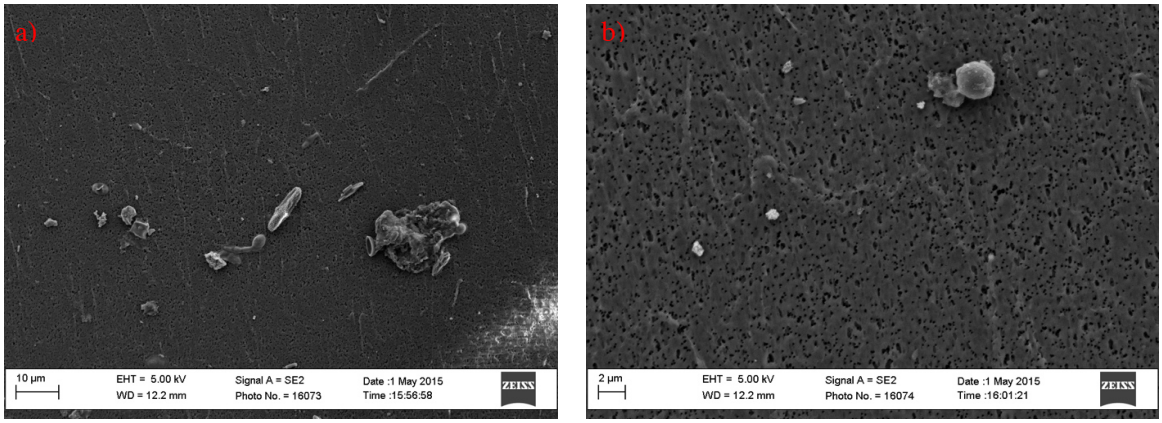

Figure 11:Scanning Electron Microscope (SEM) pictures taken of April 14, 2015 SpinCon II sample. a) shows a heterogeneous population of particles including: dust, bacteria, fungal spores and other particles; b) shows small dust particles and a small fungal spore (~2μm).

The LNA subpopulation showed FSC-A and SSC-A properties similar to bacteria isolates previously analyzed by FCM. Also, showed a 1-3 μm mean size based on the FSC-A intensity. It is clear that heterogeneous populations will contain multiple types of microorganisms and that may be the case in the LNA population. Bacteria, fungal spores and pollen are the main biocomponents of atmospheric aerosol. It has been shown that pollen breaks apart into tiny fragments when suspended in water (Augustin et al., 2012; Taylor et al., 2007). Based on such studies, pollen fragments may be present in the LNA population. However, FCM pure culture experiments suggest a 1:2 pollen-to-pollen fragments ratio (look section 3.5). Given pollen particle concentration in our samples are two orders of magnitude lower than bacteria concentration, pollen fragments are considered negligible to the bacteria quantification. Bacteria counts were quantified by a quadrant analysis performed to the LNA population based on a previously determined fluorescence threshold (3.2 K, 2.8 K), which ensures that at least 95% of unstained

particles stay below the fluorescent threshold (see Figure 12a). Bacteria subpopulation total counts is given by the sum of quadrants Q5 and Q6 in Figure 12b, which then is used in Equation 1.

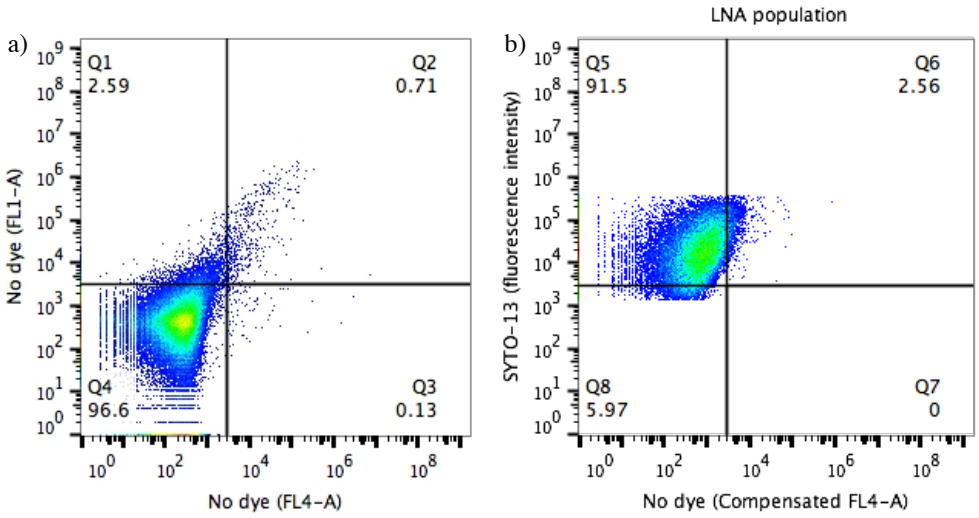

Figure 12: FL1-A vs. FL4-A plots: a) shows the threshold applied to atmospheric samples and the quadrant analysis performed to blank without SYTO-13; b) shows the LNA population quadrant analysis for bacteria quantification.

A highly fluorescent big particle subpopulation (pollen subpopulation in Figure 9) with 15 - 25 μm mean size was identified and showed substantial autofluorescence when SYTO-13 was not added to the sample, as shown in Figure 13. Pollen autofluorescence is substantially higher among bioaerosols due to specific fluorophores (i.e., phenolic compounds and carotenoid pigments) in their cell wall (Pöhlker et al., 2013; Pöhlker et al., 2012). As well, Pöhlker et al., 2013 showed pollen autofluorescence is different from that of bacteria and fungal spores, since it is associated with cell wall fluorophores and not proteins or other cytosolic compounds. The subpopulation was not well defined for two fundamental reasons: (i) Low concentration (10^2 part./m^3) compared to the other subpopulations and (ii) SpinCon II low collection efficiency for big particles. It was

quantified taking in consideration previous reasons and understanding gives us the lower bound of pollen concentration in the atmosphere.

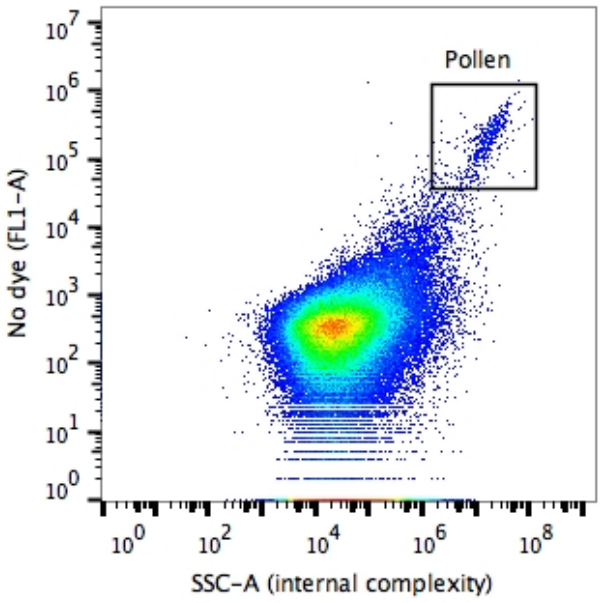

Figure 13: Pollen autofluorescence in the atmospheric sample without SYTO-13.

SYTO-13 has been effective staining bacteria RNA and DNA. Experiments performed by Guindulian et al., 1997, with seawater samples during starvation, suggest SYTO-13 could be used to differentiate bacterioplankton populations with different DNA contents without the potential interference of the variable amounts of intracellular RNA. As well, during the study they applied DNAse and RNAse to seawater samples and concluded that most of the digested genetic material was related to DNA, suggesting SYTO-13 fluorescent intensity is related to the amount of DNA in the microorganisms. During starvation, microorganisms have limited resources to perform metabolic activity, which cause them to reduce their intracellular RNA and protect their DNA. Moreover, Guindulian et al., 1997 pure culture experiments show that during starvation SYTO-13

fluorescence intensity is reduced significantly, suggesting RNA and DNA quantity reduction. In this study we performed FCM experiments with bacteria, pollen and yeast pure culture mixture. Results indicated pure cultures have an order of magnitude higher fluorescence intensity than atmospheric samples. In addition, indicate that atmospheric microbes could be subject to a stress similar to starvation causing a reduction in their genetic material. However, more work needs to be done to understand the possible genetic material degradation in microbes. Based on Guindulian et al., 1997 results, we understand that the subpopulations identified above can be differentiated based upon their DNA content.

Equation 2 was used to calculate subpopulations liquid basis concentration in the atmospheric samples, which is a modification to Lange et al., 1997 quantification equation:

$$C_{liq} = \left(\frac{subpopulation\ counts * volume\ of\ beads\ added * beads\ original\ concentration}{0.99 * AS\ aliquot\ volume * \ beads\ counts}\right) \quad [2]$$

where C_{liq} is the subpopulation concentration and the 0.99 factor takes in consideration the 10 μL of 37 wt.% formalin added to the original sample, representing a 1% dilution of the atmospheric sample aliquot volume. Beads original concentration during these experiments was 2 x 10^7 beads/mL. Then, equation 3 was applied to compute the air basis concentration of each subpopulation C_{air}:

$$C_{air} = \left(\frac{C_{liq} * sample\ total\ volume}{Spincon\ II\ sampling\ flowrate * sampling\ time}\right) \quad [3]$$

Finally, the TBAP concentration for each event was calculated by the addition of the bacteria, fungal spores and pollen subpopulations concentration.

3.1.2 FCM Subpopulations Particle Size Determination

Calibration beads FSC-A, SSC-A and FL1-A geometric mean data calculated by FlowJo was averaged. Then FSC-A results were plotted versus the beads size with its respective standard deviation reported by the supplier. A power regression, shown in Figure 14, was performed to the beads size vs. beads FSC-A intensities plot to get an equation capable of relate populations particle size with its respective geometric mean FSC-A intensity.

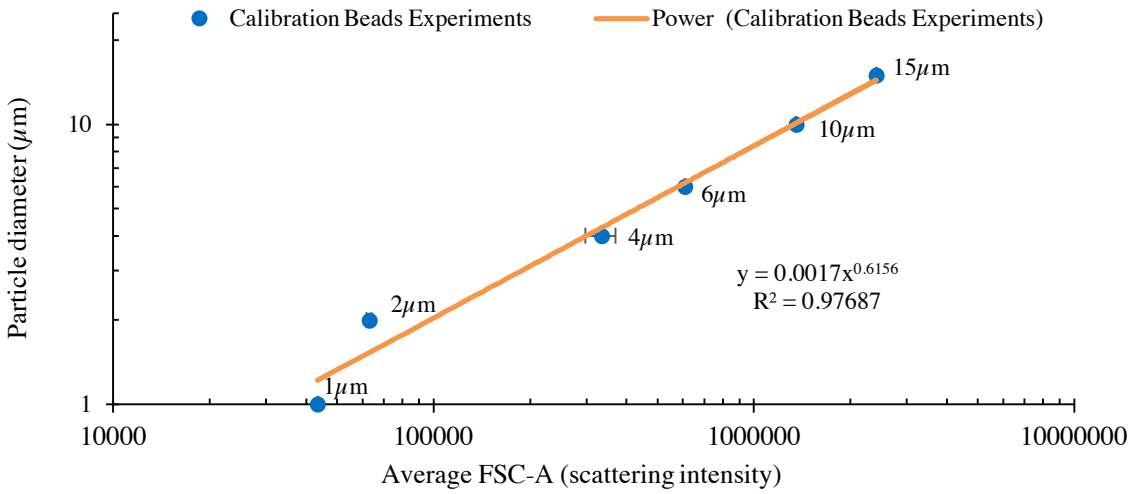

Figure 14: Plot used to determine the subpopulations mean size. Results of the FCM analysis with the calibration beads. Both axes are in logarithmic scale.

Based on the regression, the following equation was used to calculate the size of the bioparticle subpopulations:

$$S(\mu m) = 0.0017 * (I)^{0.6156} \qquad [4]$$

where S is the subpopulation mean size in μm and I is the averaged geometric mean FSC-A intensity of the subpopulation. The equation calculated the mean sizes of the distributions successfully, but it may have overestimated pollen size given the extrapolation performed to apply the equation to bigger particles. Results summarized in Table 1 describe averaged sizes of each subpopulation during April to May sampling events.

Table 1: Summary of bioparticles subpopulation sizes over April to May sampling episodes. Average size calculations were performed using equation 4.

	Bacteria	***Fungal Spores***	***Pollen***
Average size (µm)	2.62	4.66	17.40
Max size (µm)	3.16	5.37	41.17
Min size (µm)	1.83	3.00	11.58
SD (µm)	0.43	0.69	6.70
CV%	16%	15%	39%

3.1.3 WIBS Data Processing

FBAP concentrations over time were calculated in a 15 min resolution, by using Gabey et al., 2010 threshold approach. For this study WIBS total particle concentration (N_{all}), FL1 concentration (total FBAP concentration) and the concentration of the particles who went over FL1 and FL3 thresholds (FL1&3) were used. FL1&3 showed lower quantification than FL1 due to the low sensitivity of FL3 toward small FBAP (0.5 – 1.5μm) particles and it may underestimate small FBAP concentration. Given PBAP in the atmosphere have substantial biological particles in 0.5 – 1.5 μm range and WIBS-4 collection efficiency is best in this range, we did not consider FL1&3 as the total FBAP concentration. However, it was useful to understand the change of FBAP populations over time under different meteorological conditions and dN/dD_p normalized size distributions were generated for N_{all}, FL1 and FL1&3. Lastly, concentration diurnal

profiles were generated for days after rain (n=4), during rain events (n=12) and dry episodes (n=17) during April to May sampling. Data collected during rainy days were defined as 'Wet'. Data obtained a day after a rainy day were designated as 'After rain'. Data collected after two days or more after a rain episode were defined as 'Dry'.

3.2 Results and Discussion

3.2.1 FCM Results

During April to May sampling episode, 15 samples were collected. Total biological particle concentration (TBAP) ranged from 1.9×10^4 to 1.9×10^5 part. /m^3 (average: 8.4×10^4 part. /m^3), bacteria concentration ranged from 9.7×10^3 to 1.7×10^5 part. /m^3 (average: 7.5×10^4 part. /m^3), fungal spore concentration ranged from 4.7×10^3 to 2.0×10^4 part. /m^3 (average: 1.1×10^4 part. /m^3), and pollen concentration ranged from 1.3×10^2 to 1.2×10^3 part. /m^3 (average: 3.6×10^2 part. /m^3), which agree with previous quantifications in urban areas. Results showed the bioaerosol population was dominated by bacteria most of the time and changed its composition during and after rain events, invigorating the fungal spore contribution to the TBAP. Bacteria, fungal spores and pollen populations represented on average 81% and 18% and 1% of the TBAP, respectively. Fungal spores were completely depleted during 3 episodes of the 15, but constituted up to 67% of the TBAP after rain events. In general, Atlanta showed a bioaerosol community with a considerable presence of fungal spores during warm and humid days and a bacteria-dominated bioaerosol community during dry days. Figure 3 shows an overview of the bioaerosol concentrations and Figure 4 shows the composition of all FCM samples during the study.

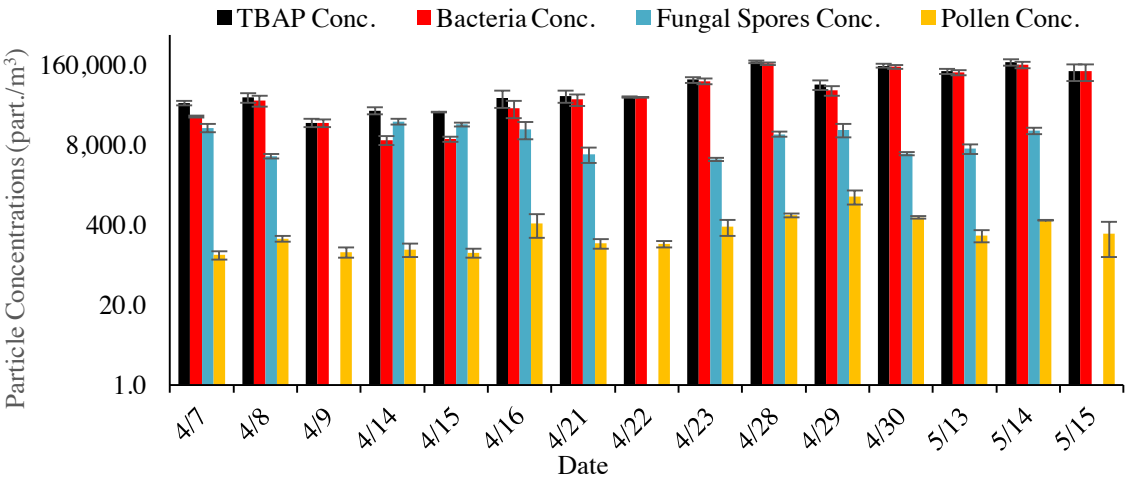

Figure 15: TBAP, bacteria, fungal spores and pollen comparative quantification summary during April to May episode. Y-axis shows bioparticles concentration in a logarithmic scale.

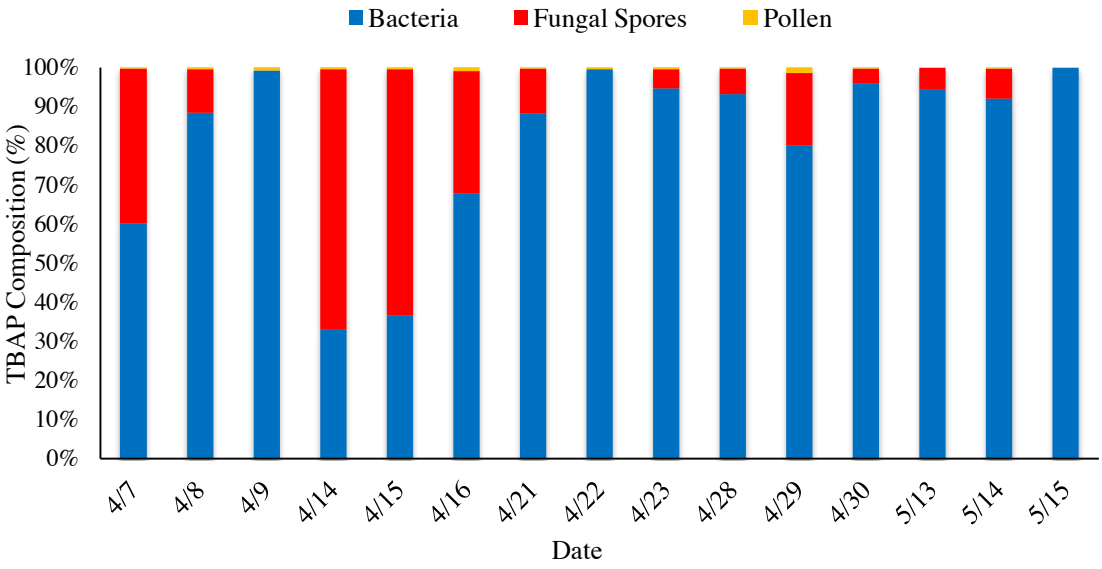

Figure 16: Bioaerosol populations composition for each sampling episode. Each composition represent a fraction of the TBAP concentration. Y-axis represents the percent (%) of each subpopulation among the TBAP concentration.

Results helped us to understand the day-to-day variability in bioaerosol communities and to compare bioaerosol subpopulations abundance under similar meteorological conditions. Based on the results, we observed different bioaerosol behavior between humid and warm episodes and dry periods. Humid and warm episodes (n=4) were defined as those with $T_{ave.} > 70°F$ and $RH_{ave.} > 50\%$, while dry episodes were defined as those with $RH_{ave.} < 50\%$. $T_{ave.}$ and $RH_{ave.}$ are the average temperature and relative humidity during the sampling time.

3.2.2 Humid and Warm Episodes

Well-defined fungal spores and LNA subpopulations characterized humid and warm episodes. During the study, six episodes were considered humid, of which four were humid and warm. We observed these episodes had significant amounts of fungal spores compared to others and the FCM technique was able to successfully detect, quantify, and track its day-to-day variability. Among humid and warm days (n=4), bacteria and fungal spores average compositions were 57% and 42%, respectively. However, among these four events, May 15nd did not detect the fungal spores subpopulation, which suggests that fungal spores may be regionally transported, rather than locally available (see Appendix A: Figure 28). Additionally, this week was dry and did not have any rain events. During the rest of the episodes (April 7th, April 14nd and April 15nd) the wind came from the south and substantial fungal spore concentrations were seen. During the sampling episodes between April 7th and April 9th, we saw a significant change in bioaerosol subpopulations compositions from a humid and warm day to a dry day (see Appendix A: Figure 26). Figure 17a-c show FL1 vs. SSC-A plots for April 14nd to April 16nd consecutive sampling episodes. This week bacteria

concentration increased as the fungal spore concentration slightly decreased. Fungal spores fraction went down from 67% to 31% of the TBAP. As well, TBAP concentration maintained between 2.8 x 10^4 to 4.7 x 10^4 part. /m^3.

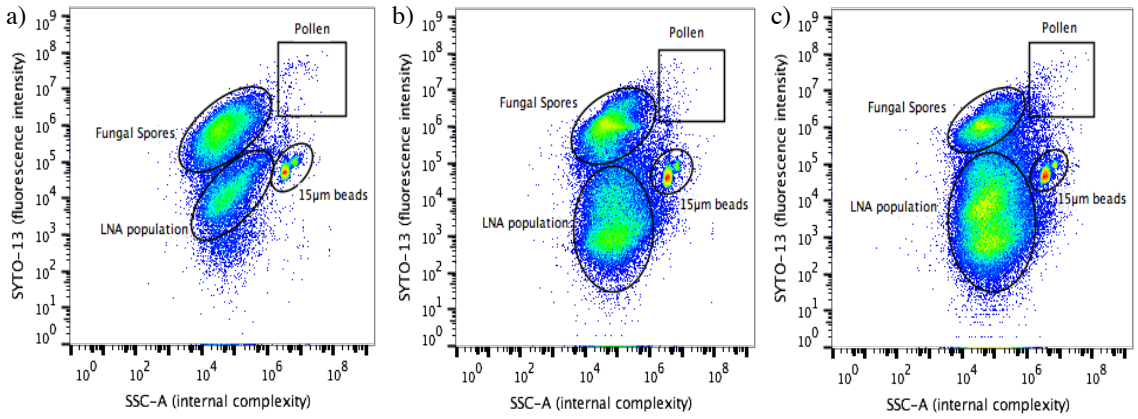

Figure 17a-c: FL1-A vs. SSC-A plots (pseudo-color plots show higher particle accumulation in green to red regions) show April 14nd to April 16nd consecutive sampling episodes during humid and warm days. Plots show a decrease in fungal subpopulation and an increase in the LNA population during the consecutive events.

3.2.3 Dry Episodes

Spring sampling was dominated by dry episodes and nine of the fifteen episodes were considered dry events. TBAP was dominated by bacteria subpopulation during these events, as we can see in Figure 18a-c, where the LNA subpopulation looks well populated. However, fungal spore number drops in Figure 18a and c and disappears in Figure 18b. Among dry days, bacteria and fungal spores average compositions were 94% and 6%, respectively. During dry periods, average bacteria concentration is two-fold higher than during wet and humid periods. In general, results show Atlanta TBAP is currently dominated by bacteria during spring and regularly these dry episodes may invigorate the amount of TBAP up to 1.8 x 10^5 part./m^3. Similar to what is seen between April 21st to April 23rd episodes, samples collected during April 28th, April 30th, May 13nd

and May 14nd show a well-defined bacteria subpopulation and a diminished fungal spore population.

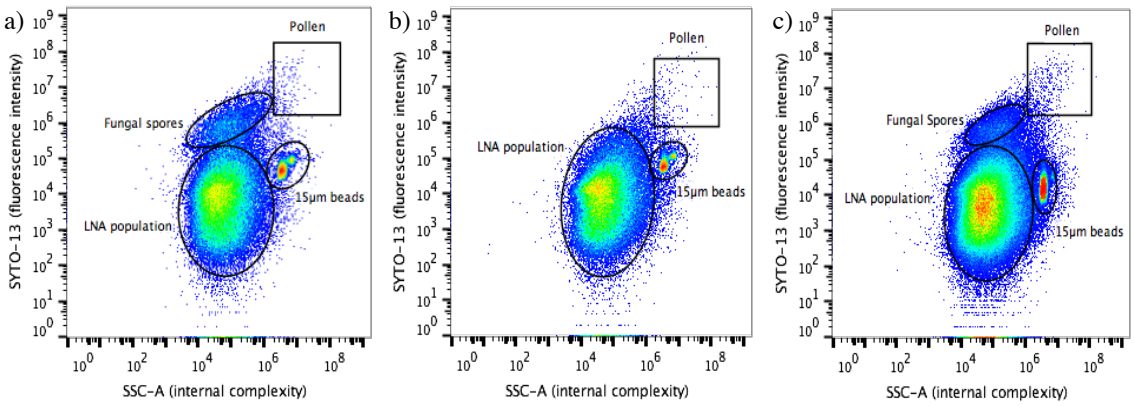

Figure 18a-c: FL1-A vs. SSC-A plots of the April 21st to April 23rd consecutive sampling episodes during dry days. Plots show the reduction in fungal spores subpopulation with respect to humid and warm days and its disappearance during April 22nd episode.

Among the diverse scenarios seen during April to May sampling, we agree the FCM protocol have been effective to detect and quantify bioaerosol subpopulations with different DNA content. Moreover, the protocol has been able to quantify the day-to-day variability of the bioaerosols in the Atlanta area and be consistent over similar meteorological scenarios. FCM analysis suggest Atlanta TBAP is mainly dominated by bacteria, but its composition may change as rain events bring humid and warm days during spring, causing a substantial increase in fungal spores. From the health perspective, this finding is quite important given, the increased probability of illness during these episodes. When atmospheric sample results are compared to pure culture samples, we observe a reduction in the atmospheric samples' SYTO-13 fluorescence intensity. The reduction may suggest a degradation of their genetic material. Atmospheric samples and pure cultures should not be directly compared, due to the more controlled environment of the laboratory. However, it is important to realize FCM could help us to

understand microbe life cycle, an important piece of information to understand bioparticles integration in clouds and its role in the hydrological cycle.

3.3 WIBS and FCM Comparison

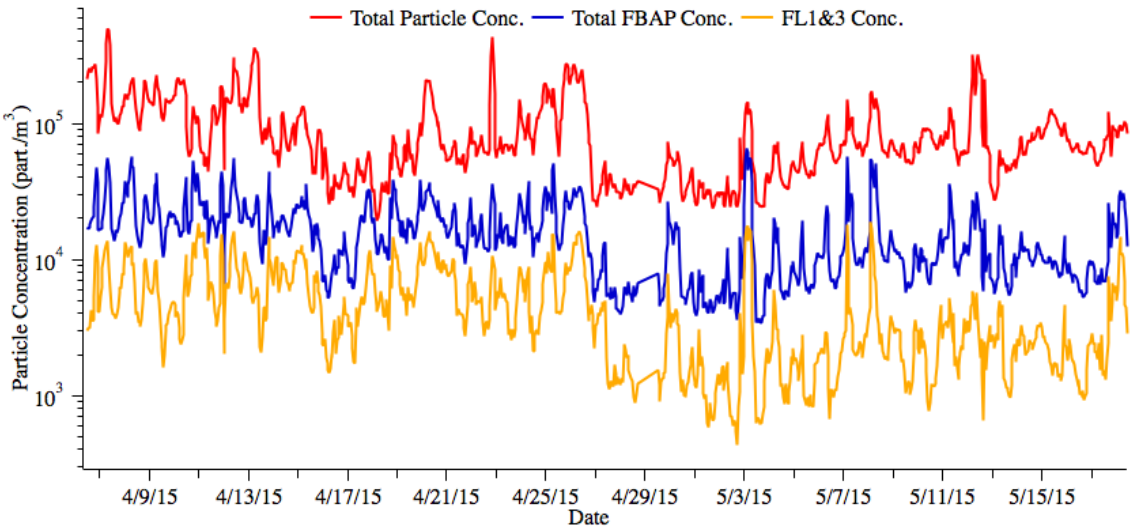

Figure 19: WIBS total particle, total FBAP and FL1&3 concentration profiles during April-May sampling. Plots show 1hr resolution results from April 6th to May 16nd.

WIBS total particle concentrations during sampling episode averaged 8.9 x 10^4 part. /m^3 (1.9 x 10^4 to 4.9 x 10^5 part. /m^3) as we can see in Figure 19. As well, the total FBAP concentration averaged 1.6 x 10^4 part. /m^3 (3.4 x 10^3 to 6.6 x 10^4 part. /m^3) and it was on average 19% of the WIBS total particle concentration. FBAP results are similar to the average TBAP seen by FCM technique in Figure 20. However, in most of the events, the TBAP concentrations are an order of magnitude higher than the total FBAP concentrations. It is understandable given that FCM is a more specific technique due to the use of a DNA probe and there should be bioparticles below the WIBS autofluorescence threshold that are not counted as FBAP. FL1&3 concentration averaged 4.8 x 10^3 part. /m^3 (4.3 x 10^2 to 1.9 x 10^4 part. /m^3) during April to May episodes and its concentration may be related to fungal spores during and after rain events. Neither FL1 or

FL1&3 concentrations were quantitatively consistent with any FCM subpopulation, but the shift in the size distribution peaks between humid and warm periods and dry periods agree with the size of the subpopulations observed by FCM.

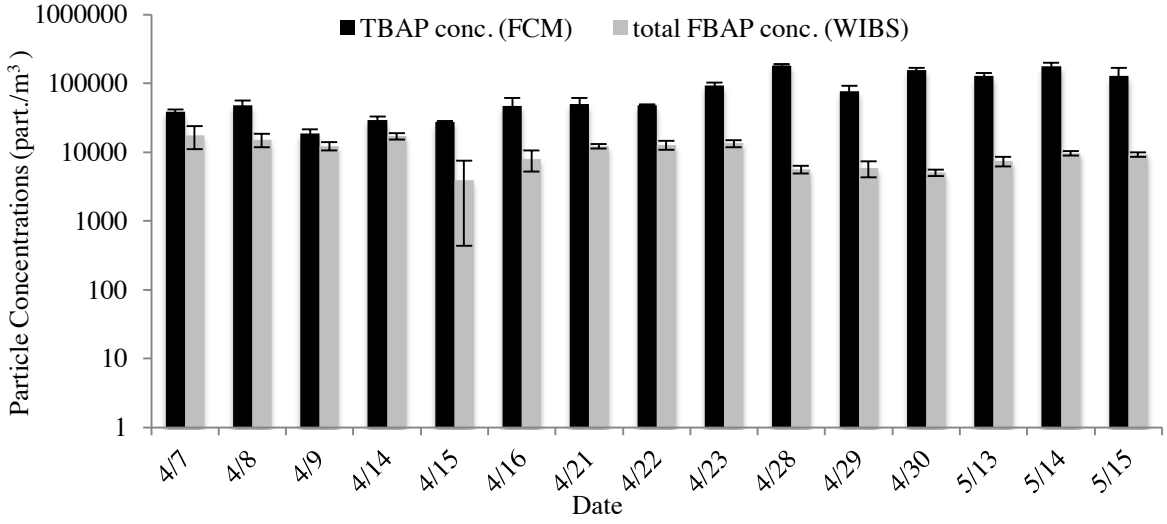

Figure 20: TBAP and total FBAP concentration comparison for April to May SpinCon II samples.

Humid and warm episodes after rain events characterized by having a strong presence of 4-7 μm bioparticles. FCM and WIBS size distributions results show similar behavior during these episodes. Figure 21 shows a persistent population of big biological particle, which increase its frequency during the night and decrease it during the day. Even when its frequency decrease around midday it persists during the whole day, as is seen in Figure 21, which may explain its detection in the SpinCon II collection between 11am-5pm. Our findings suggest fungal spores may maintain elevated concentrations up to 24hrs after the rain event. Furthermore, these findings agree with Huffman et al., 2013 study in the Rocky Mountains, Colorado after rain events. They found the number fraction of FBAP in the supermicron range detected by the UV-APS was as high as 40%

during humid conditions after a strong daytime precipitation; and that 4-6 μm fluorescent bioparticles appeared 8 hours after the precipitation and persisted for up to 12 more hours. Additionally, diurnal cycles in Figure 23 show FBAP concentration is higher during and after rain events than during dry events. As well, the diurnal cycles suggest fungal spores active wet ejection at elevated relative humidity (Després et al., 2012; Elbert et al., 2007) given FL1 and FL1&3 notable increase during nighttime. Even when Atlanta is an urban area, it is surrounded by several forests that may influence the availability of biological particles supporting a similar behavior to highly vegetative areas as result of biological particles transport to the city.

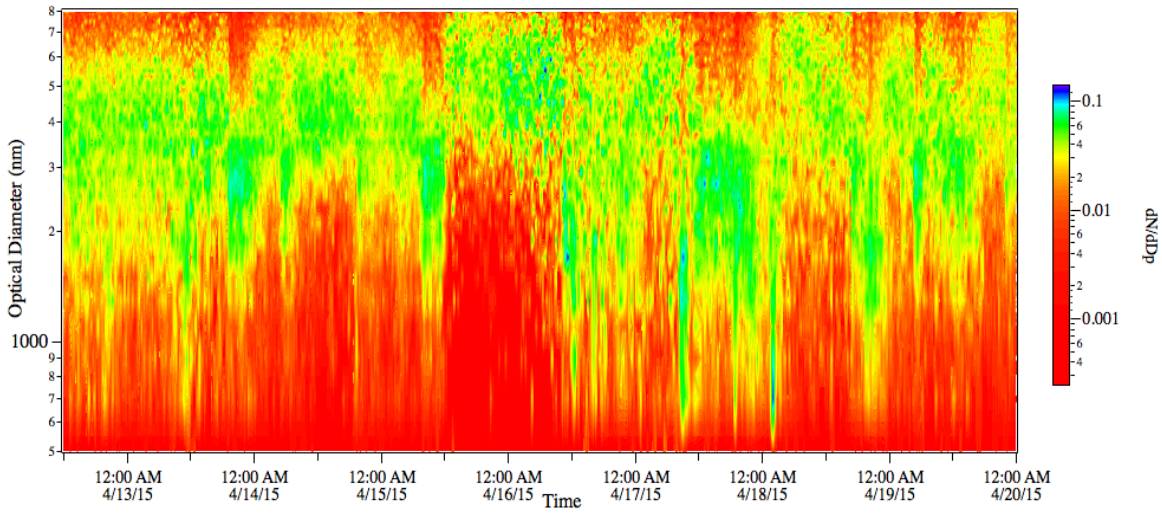

Figure 21: FL1&3 normalized size distribution profiles during April 14nd and April 16nd SpinCon II sampling events. Contour plot has a 15min resolution and the color bar in the right represents the frequency of occurrence (green and blue areas represent the peak of the distributions).

During dry episodes, fungal spore subpopulation decreased its concentration substantially and was depleted in several episodes, including the episode which occurred on April 22nd. WIBS FL1&3 size distributions in Figure 22 showed a significant reduction in the frequency of big particles between April 21st and April 23rd, and a change in the size distribution peak toward 1-3 μm size particles. Moreover, the peak is

consistent and it agrees with the size of the well-defined bacteria subpopulation seen by FCM. As well, the diurnal cycles seen in Figure 23 show similar behavior to that observed by Gabey et al., 2011 in Manchester. Also, the diurnal profiles show an early morning and after sunset concentration peaks, which suggest a non-fungal spores dominated atmosphere. As result, understand under dry conditions Atlanta bioaerosols may be dominated by bacteria or other 1-3 μm bioparticle subpopulation.

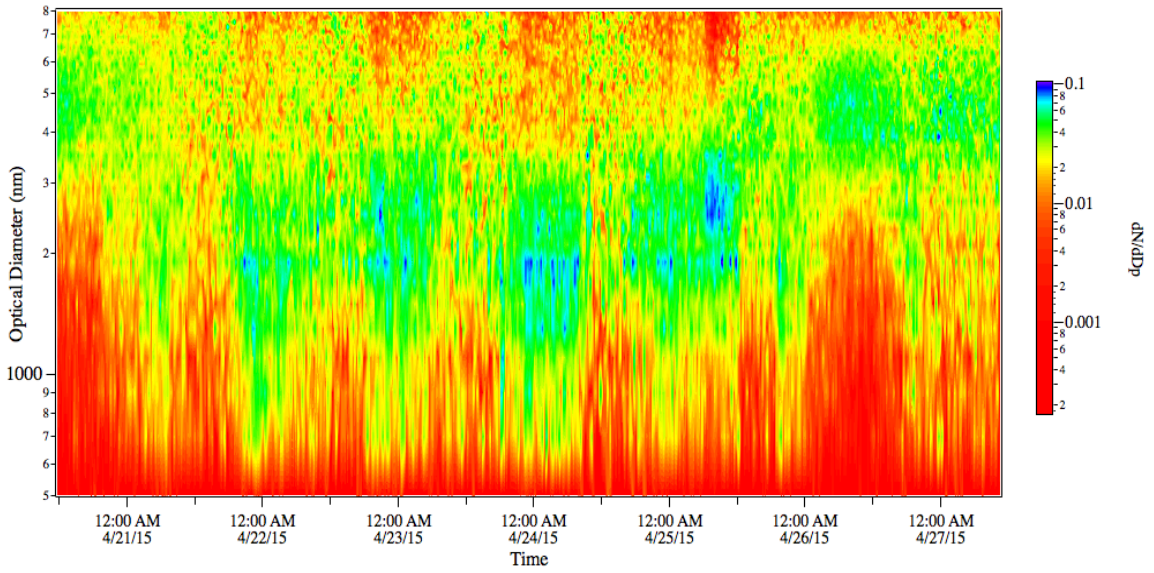

Figure 22: FL1&3 normalized size distribution profiles during April 21st and April 23rd SpinCon sampling events. Contour plot has a 15min resolution and the color bar in the right represents the frequency of occurrence (green and blue areas represent the peak of the distributions).

Diurnal cycles in Figure 23 show qualitative similarities to previous studies, as discussed above, but the total FBAP concentration difference between "After Rain" and "Dry" diurnal cycles is not quantitatively significant during the sampling time (11am to 5pm Atlanta local time). The small difference in the total FBAP concentration may be a result that Atlanta is a non-fungal spores dominated ecosystem and bacteria or other bioaerosols could play an important role. However, FL1&3 "After Rain" diurnal profile concentrations (look appendix A Figure 35) are up to 2 folds higher than "Dry" events

concentration during the sampling time, which in fact suggest a possible change in the composition of the PBAP even when the total FBAP concentration is not changing drastically.

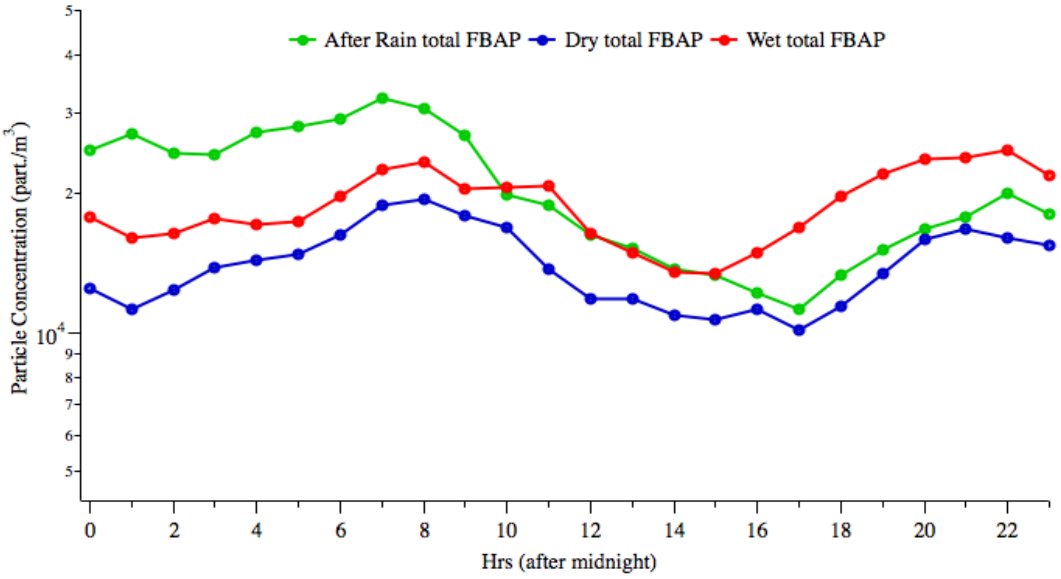

Figure 23: WIBS total FBAP concentration average diurnal profiles for after rain (n=4), during rain (n=12) and dry (n=17) episodes during April to May sampling.

In general, we should understand FCM and WIBS give us two different type of data. FCM gives a batch type quantification of the TBAP for the four hours SpinCon II collected particles. However, WIBS gives us time series concentrations of FBAP. Each technique has its biases, but together gives us valuable information. From the molecular perspective, we agree there are two main subpopulations in the biological samples with different amount of genetic material. At the same time, WIBS and FCM agree on their population particle size. Moreover, the diurnal profiles give additional information about its daily behavior and its link to meteorology gives an idea of how they may be interacting with the atmosphere.

3.4 Additional Atmospheric Samples: September 2015 Sampling

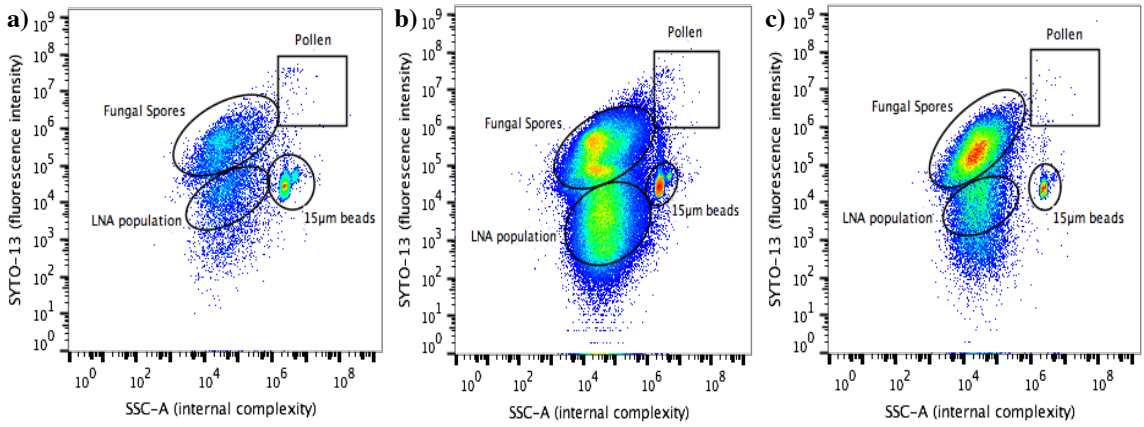

Figure 24a-c*:* FL1-A vs. SSC-A plots of the September 9th to September 11nd consecutive sampling episodes during humid and rainy days. a) shows the reduction in biological particles abundance during a rain event; b) shows an invigoration in biological particles during the beginning of a rain event in September 10th; and c) shows the invigoration of fungal spores after a rain event.

Additional atmospheric samples were collected during rainy days between September 9th and September 11nd to get a better understanding of the invigoration in the fungal spore subpopulation and look additional cases of humid and warm events. Samples were analyzed using the same protocols that used for April to May samples, but during the collection, WIBS-4 was not acquiring data. The three consecutive episodes can be considered as humid and warm given its high relative humidity and temperature. As well, similar to the humid and warm days in April to May sampling, southern and southeastern winds predominated. Overall, fungal spores dominated by being between 63% to 80% of the TBAP and its concentration reached 2.8 x 10^5 part. /m^3 after the rain event in September 11nd (Figure 24c). However, during the rain event in September 9th (Figure 24a) the TBAP concentration went down to 6.6 x 10^3 part. /m^3, which may be an effect of the particles wet deposition by the rain. Results seen in September support the April to May sampling. Observations suggest southern winds could carry biological

particles to the city of Atlanta, and the biological particles are aerosolized in a substantial amount during humid and warm days after rain events.

3.5 FCM Pure Cultures Experiments

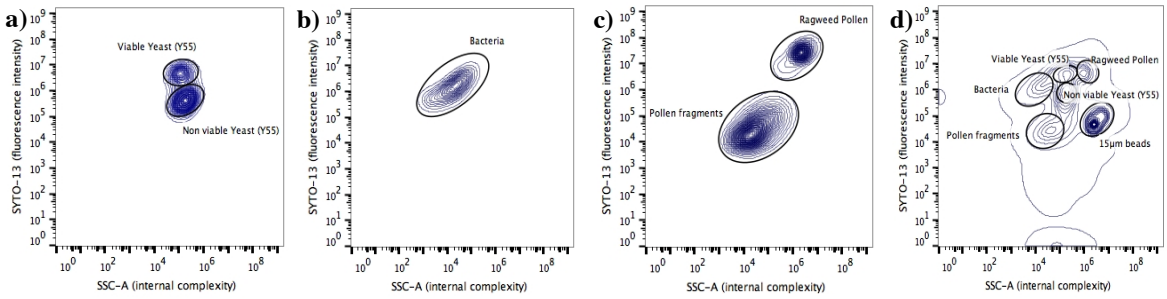

Figure 25: Pure Cultures FL1-A vs. SSC-A results. a), b) and c) show FCM results of individual yeast (Y55), bacteria atmospheric isolate (F8), and Ragweed pollen, respectively; and d) shows FCM results of the microorganism mixture.

As described in the pure culture methodology section, two types of experiments were performed: i) individual pure cultures and ii) pure cultures mixture experiments. Figure 25a-c show the results of the individual microbial populations. Results in Figure 25d show subpopulations are close to each other given their similar sizes and internal complexities. Also, microorganism subpopulations show higher SYTO-13 fluorescence intensity than those in the atmospheric samples, as it is observed in Figure 25a-d and summarized in Table 3. Among mixed populations experiment we focused in the pollen to pollen fragments ratio given pollen fragments importance in the atmospheric bacteria quantification. Based on the results, a 1.1 x 10^4 part. /mL pollen population will release 2.7 x 10^4 part. /mL of pollen fragments when is in contact with aqueous solution, which constitute approximately a 1 to 2.4 ratio (Look Table 2). As result, given the small pollen concentrations seen in the atmospheric samples understand the impact of pollen fragmentation in atmospheric bacteria quantification will be negligible.

Table 2: Pure cultures triplicate concentrations overview. SC1880, SC1881 and SC1882 acronyms are used to represent the statistical triplicate of the pure culture mixture experiment.

	Pure Culture Triplicates			Conc. Average (part. /mL)	SD (part. /mL)	CV (%)
	SC1880	**SC1881**	**SC1882**			
Pollen Conc.	1.20E+04	1.04E+04	1.05E+04	1.09E+04	8.96E+02	8.2%
Pollen Fragments Conc.	2.92E+04	2.27E+04	2.78E+04	2.66E+04	3.41E+03	12.8%
Bacteria Conc.	1.99E+04	1.75E+04	1.55E+04	1.76E+04	2.23E+03	12.6%
Viable Yeast Conc.	2.61E+04	2.45E+04	2.57E+04	2.54E+04	8.37E+02	3.3%
Non-Viable Yeast Conc.	4.09E+04	4.25E+04	3.65E+04	4.00E+04	3.13E+03	7.8%

Pure culture and atmospheric samples results show interesting differences in their fluorescence intensities, which may be related to a reduction of the atmospheric microorganisms' genetic content due to the starvation caused by atmospheric stressors. Pure cultures and atmospheric samples FSC-A, SSC-A and FL-1 properties are summarized in Table 3 and Table 4, respectively. Bacteria atmospheric subpopulation shows a FL1-A intensity two order of magnitude lower than F8 bacteria. As well, fungal spore atmospheric subpopulation shows FL1-A intensity an order of magnitude lower than Y55 yeast. However, pollen subpopulations have a similar FL1-A intensity and Figure 25c shows its FL1-A intensity may go up to 10^8. The fluorescence intensity differences may be related to the capability of each group of microorganisms to resist atmospheric stressors and hold genetic material degradation given their different physiological characteristics.

Table 3: Pure cultures mixture FSC-A, SSC-A and FL1-A properties summary.

	FSC-A Avg.	*FSC-A SD*	*SSC_A Avg.*	*SSC-A SD*	*FL1-A*	*FL1-A SD*
Bacteria	7.23E+04	8.54E+03	1.52E+04	2.67E+03	1.30E+06	1.80E+05
Viable yeast	6.03E+05	1.08E+04	1.45E+05	9.45E+03	4.04E+06	1.66E+05
Non-viable yeast	1.17E+06	2.08E+04	1.61E+05	4.08E+03	6.16E+05	1.43E+05
Pollen	5.03E+05	9.50E+03	8.72E+05	3.95E+04	4.21E+06	2.54E+05
Pollen fragments	7.54E+04	4.77E+03	4.27E+04	1.44E+04	2.47E+04	8.47E+02

Table 4: Atmospheric subpopulations FSC-A, SSC-A and FL-1 properties summary during April to May sampling.

	Bacteria Geo Mean			***Fungal Spores Geo Mean***			***Pollen Geo Mean***			***Beads Geo Mean***		
	FSC-A	SSC-A	FL1-A	FSC-A	SSC-A	FL1-A	FSC-A	SSC-A	FL1-A	FSC-A	SSC-A	FL1-A
Average	1.53E+05	7.14E+04	1.39E+04	3.88E+05	7.83E+04	6.64E+05	3.52E+06	5.83E+06	6.50E+06	3.03E+06	3.28E+06	5.90E+04
SD	3.42E+04	1.84E+04	3.57E+03	8.51E+04	2.98E+04	2.26E+05	2.81E+06	5.83E+06	3.00E+06	6.30E+05	7.50E+05	4.35E+04
Max	2.12E+05	1.10E+05	2.31E+04	4.90E+05	1.31E+05	1.10E+06	1.41E+07	2.89E+07	1.61E+07	4.12E+06	4.96E+06	2.15E+05
Min	6.70E+04	2.24E+04	7.79E+03	1.65E+05	1.97E+04	2.90E+05	1.56E+06	2.28E+06	1.97E+06	1.67E+06	1.86E+06	1.35E+04

CHAPTER 4

CONCLUSIONS

Along this manuscript, we have shown the design and testing of an effective FCM protocol to identify and quantify different bioaerosol subpopulations. The FCM protocol is designed to constrain any particle accumulation due to cleaning or by fluid supplies. It represents the first study in which well-defined LNA and HNA atmospheric microbial populations have been detected and studied under different meteorological scenarios by FCM. Moreover, it has been successful to understand the change in microbial abundance and composition during regular dry days and humid and warm days after rain events. Results agree there is a significant change in the bioaerosol composition of Atlanta during humid and warm days after rain events that leads to a 42% and 57% of fungal spores and bacteria in the TBAP, respectively. In addition, September 2015 FCM experiments during rain events support the observations seen during April to May sampling episodes. Results suggest an invigoration in the contribution of the fungal spore subpopulation to the TBAP after rain events when southern winds predominated. However, during dry conditions bacteria dominates with a 94% of the TBAP.

WIBS supported FCM results by showing diurnal profiles during wet and humid episodes similar to previous linked to highly vegetative and fungal spores dominated areas. Also, WIBS shift in the peak of the size distributions mimics the predominant 1-3 μm FCM bacteria subpopulation during dry days. Ultimately, the TBAP and total FBAP concentrations represent the upper and lower bounds of the total PBAP concentration, respectively.

Additional FCM experiments with pure culture mixtures show yeast, bacteria and pollen will be a complex biological particles population to analyze because of their size and internal complexity similarities. Pure cultures showed higher SYTO-13 fluorescent intensities than atmospheric samples, suggesting atmospheric stressors may cause bioparticles genetic material degradation like a starvation process.

In summary, the combination of the FCM and WIBS techniques has given us a more complete information of the abundance, composition, possible DNA content and diurnal variability of different bioaerosol subpopulations in Atlanta. We understand the design of the protocol and its application is a significant step to make bioaerosol quantification less uncertain, more specific and less time consuming. However, bioparticles' lifecycle has been a difficult challenge in the field and FCM may have the capability to tag specific cells, as more specific biomarkers are tested in atmospheric samples.

APPENDIX A: ADDITIONAL PLOTS

TBAP Quantification

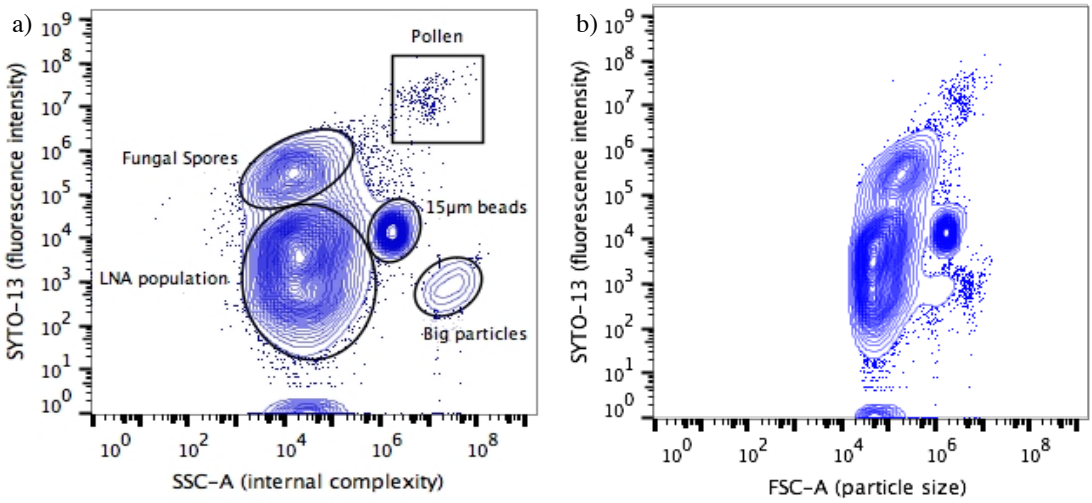

Figure 26: FLI-A vs. SSC-A contour plots used in subpopulations gating using Flow Jo software maximum resolution (2% contour plots).

FCM Atmospheric Samples Plots

April 7-9, 2015 Episodes

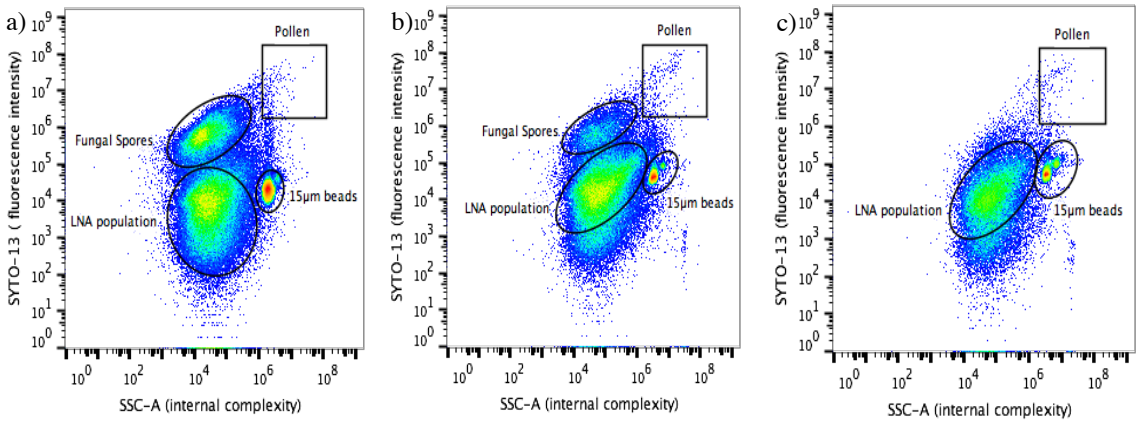

Figure 27: FL1-A vs. SSC-A plots (pseudo-color plots show higher particle accumulation in green to red regions) show April 7th to April 9th consecutive sampling. a) shows the well-defined fungal spore population during a warm and humid day. b) shows the decrease in the fungal subpopulation during April 8th and c) its depletion as dry days arrive in April 9th.

April 28-30, 2015 Episodes

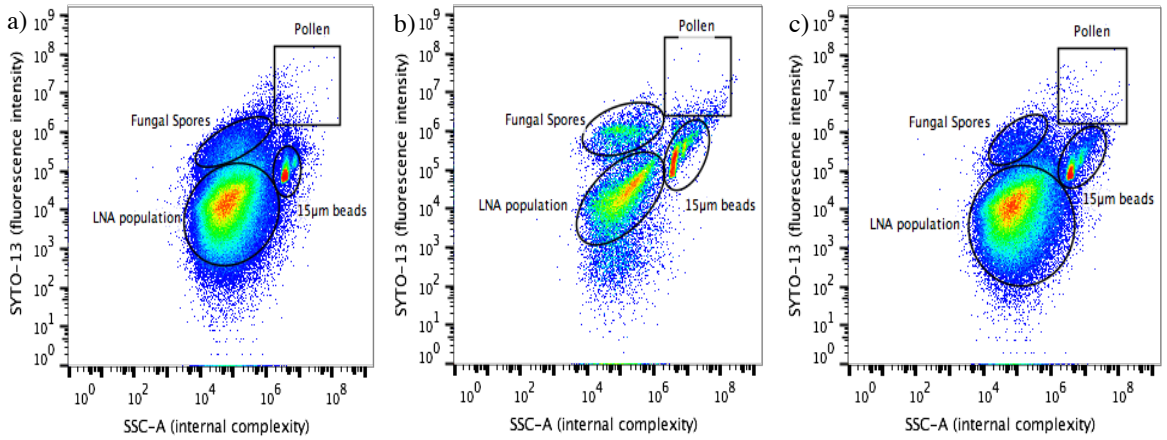

Figure 28: FL1-A vs. SSC-A plots (pseudo-color plots show higher particle accumulation in green to red regions) show April 28th to April 30th consecutive sampling. a) shows a dry episode, b) is a rainy episode with a slightly invigoration of fungal spores (short rain episode) and c) is a dry day after a rain event.

May 13-15, 2015 Episodes

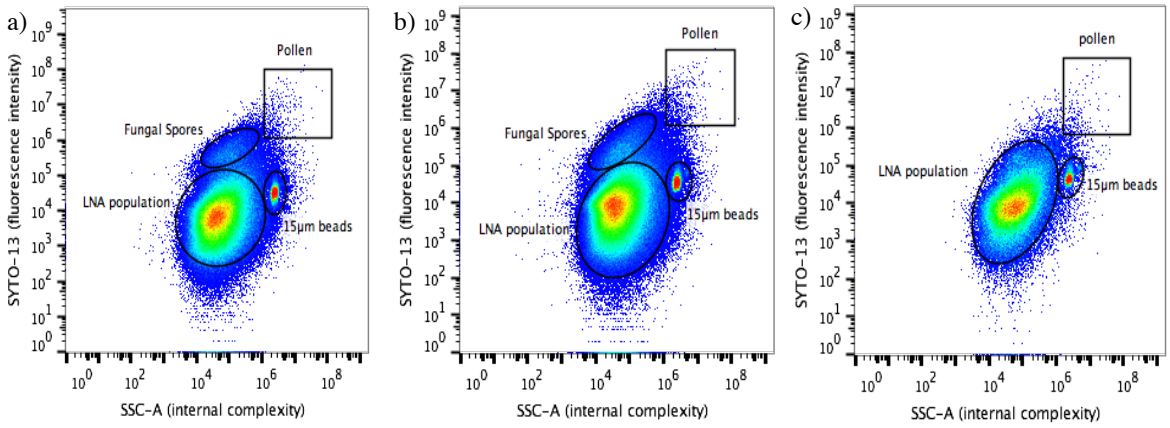

Figure 29: FL1-A vs. SSC-A plots (pseudo-color plots show higher particle accumulation in green to red regions) show May 13nd to May 15nd consecutive sampling. a) and b) show two dry days with well-defined LNA populations; and c) show a "humid and warm" episode with a depleted fungal spore population (wind blowing from the east during this episode).

WIBS Size Distributions

Week: April 12-20, 2015

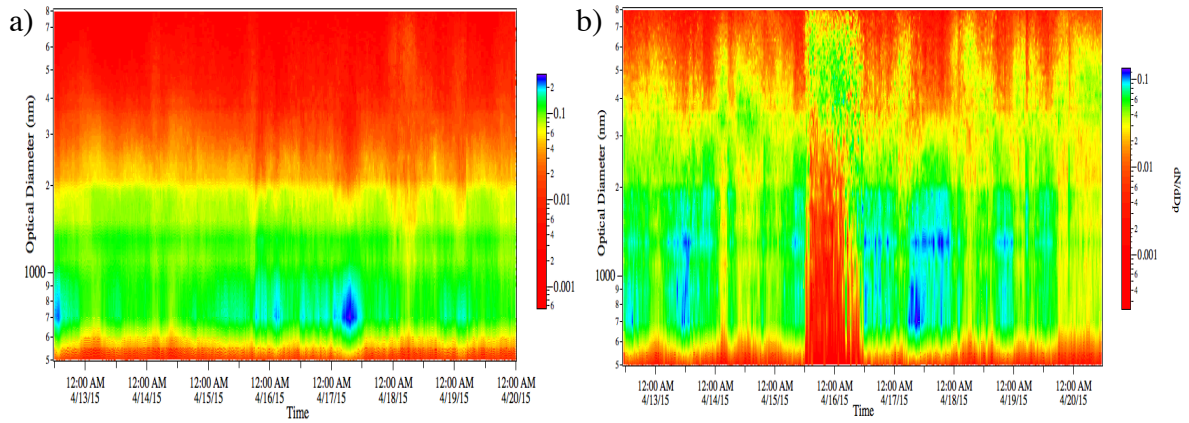

Figure 30: WIBS normalized size distribution profiles between April 12th and April 20th. a) shows the total WIBS particle concentration and b) shows the total FBAP concentration (based on FL1) size distributions. Contour plots have a 15 min resolution and the color bar in the right represents the frequency of occurrence (green and blue areas represent the peak of the distributions).

Week: April 20-26, 2015

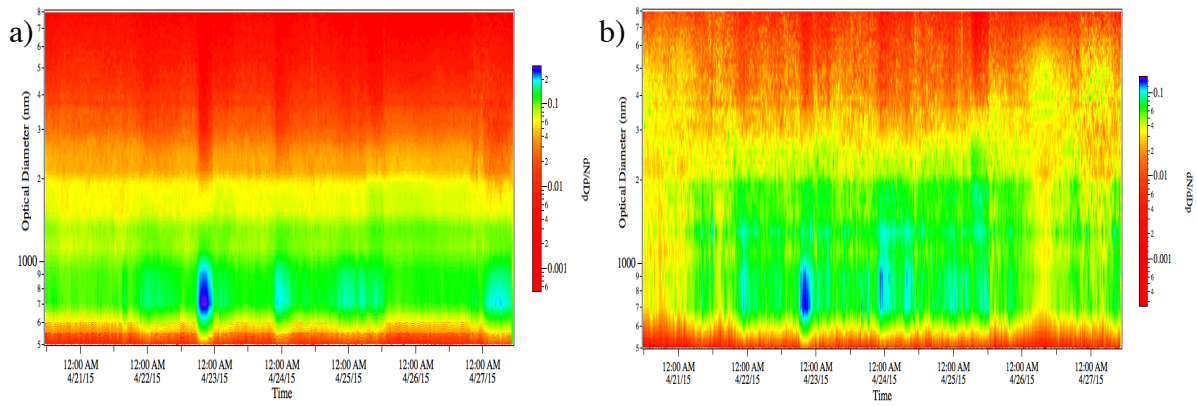

Figure 31: WIBS normalized size distribution profiles between April 20th and April 27th. a) shows the total WIBS particle concentration and b) shows the total FBAP concentration (based on FL1) size distributions. Contour plots have a 15 min resolution and the color bar in the right represents the frequency of occurrence (green and blue areas represent the peak of the distributions).

Week: April 5-12, 2015

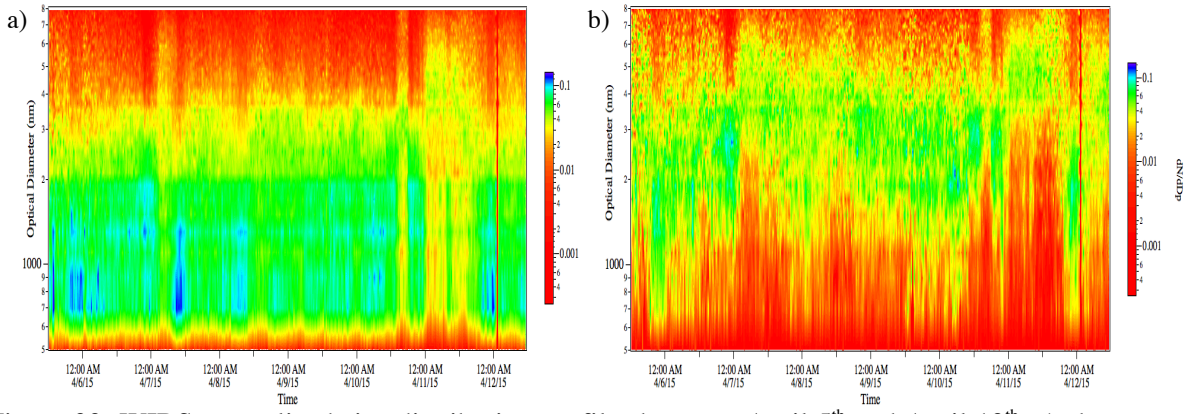

Figure 32: WIBS normalized size distribution profiles between April 5th and April 12th. a) shows the total FBAP concentration (based in FL1) and b) shows the FL1&3 concentration size distributions. Contour plots have a 15 min resolution and the color bar in the right represents the frequency of occurrence (green and blue areas represent the peak of the distributions).

Week: April 27 – May 3, 2015

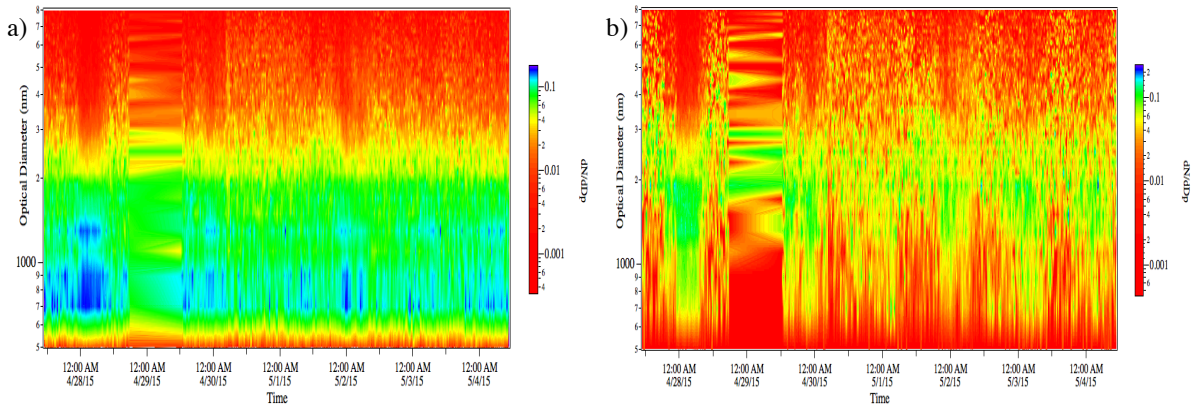

Figure 33: WIBS normalized size distribution profiles between April 27th and May 4th. a) shows the total FBAP concentration (based in FL1) and b) shows the FL1&3 concentration size distributions. Contour plots have a 15 min resolution and the color bar in the right represents the frequency of occurrence (green and blue areas represent the peak of the distributions). ***During this week WIBS-4 did not sample from April 29th afternoon until April 30th midday due to power outage*.

Week: May 10-17, 2015

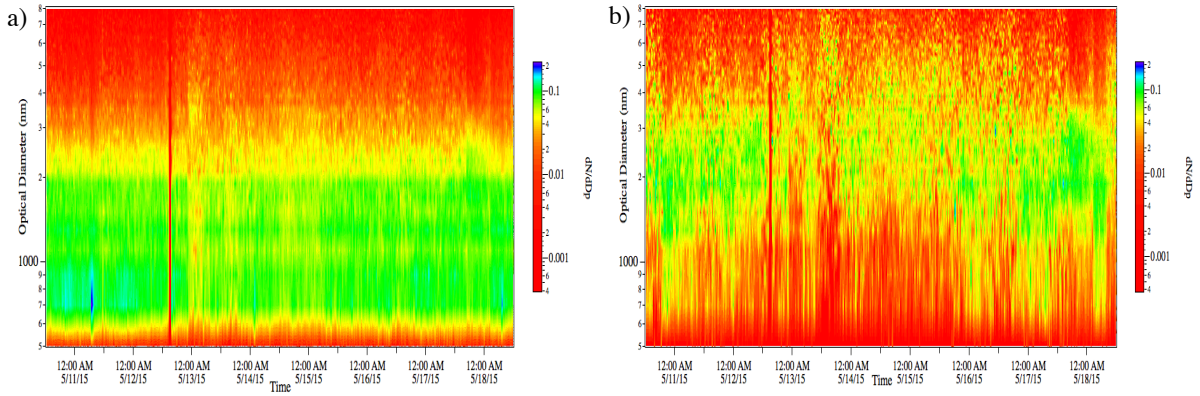

Figure 34: WIBS normalized size distribution profiles between May 10th and May 18nd. a) shows the total FBAP concentration (based in FL1) and b) shows the FL1&3 concentration size distributions. Contour plots have a 15 min resolution and the color bar in the right represents the frequency of occurrence (green and blue areas represent the peak of the distributions).

FL1&3 Diurnal Profiles

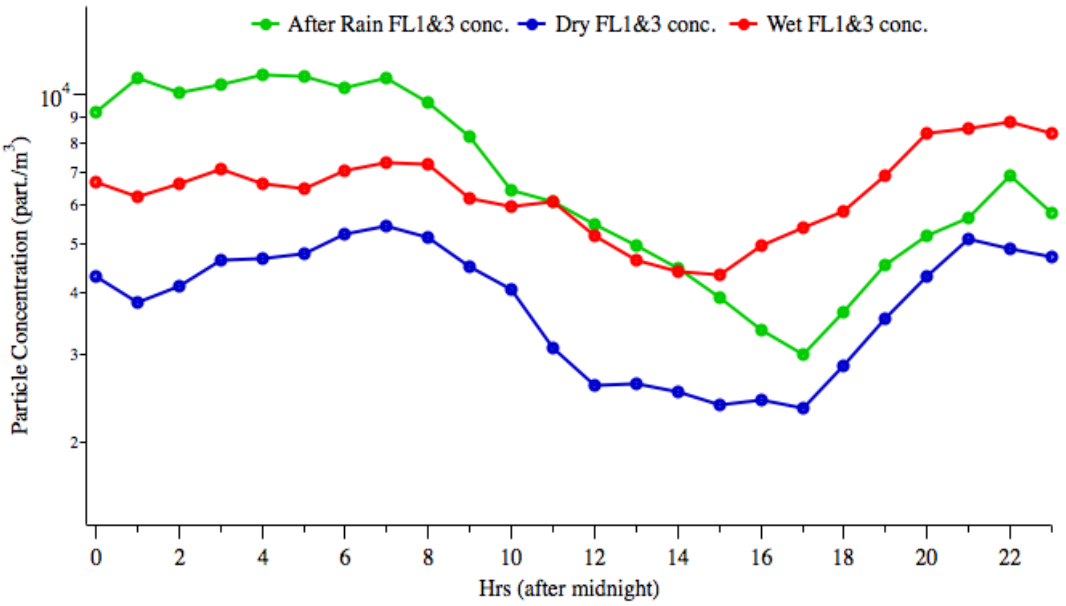

Figure 35: WIBS FL1&3 concentration average diurnal profiles for after rain (n=4), during rain (n=12) and dry (n=17) episodes during April to May sampling.

Meteorological Data

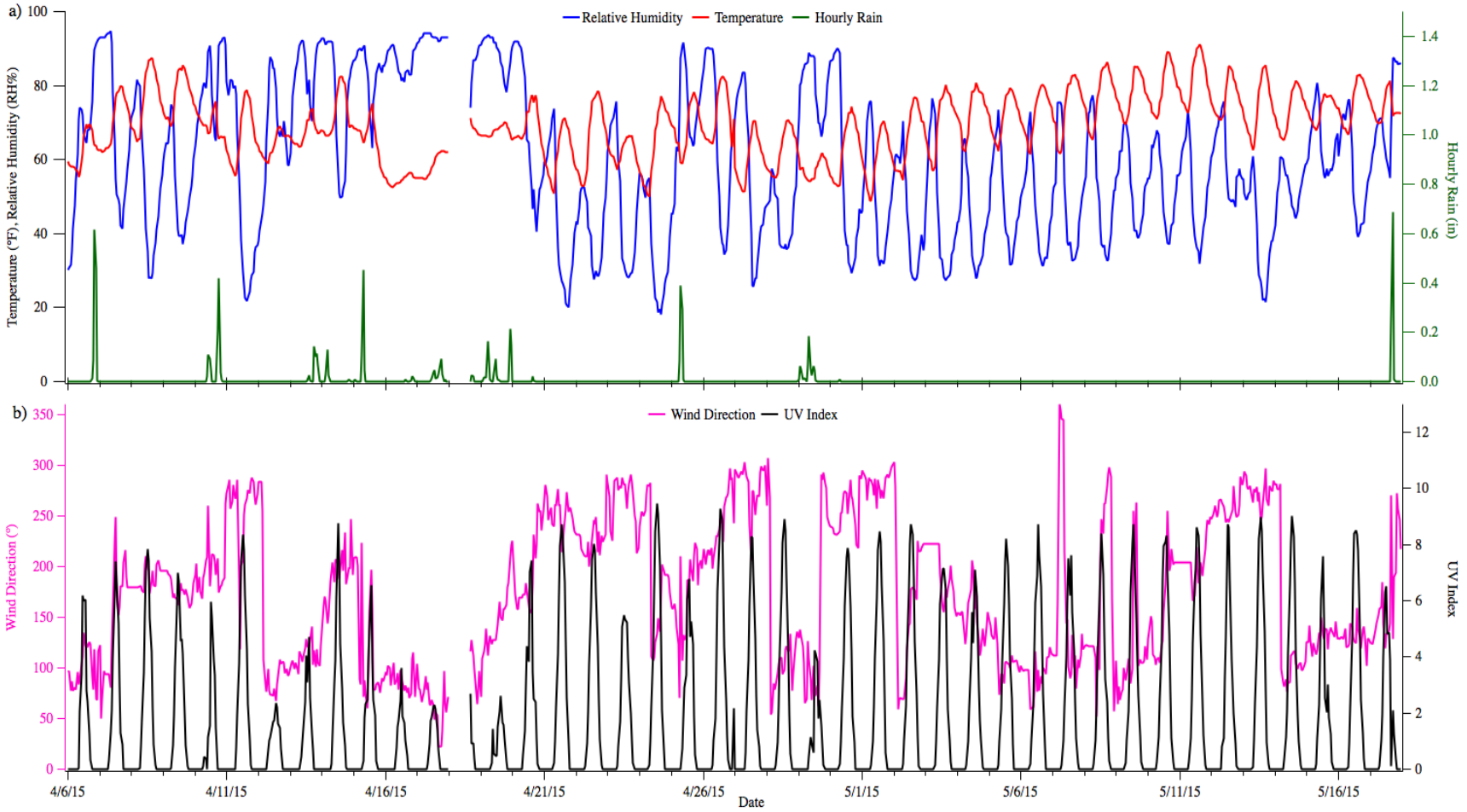

Figure 36: April to May meteorological data summary (hourly averages). It includes relative humidity, temperature, hourly rain, wind direction and UV index.

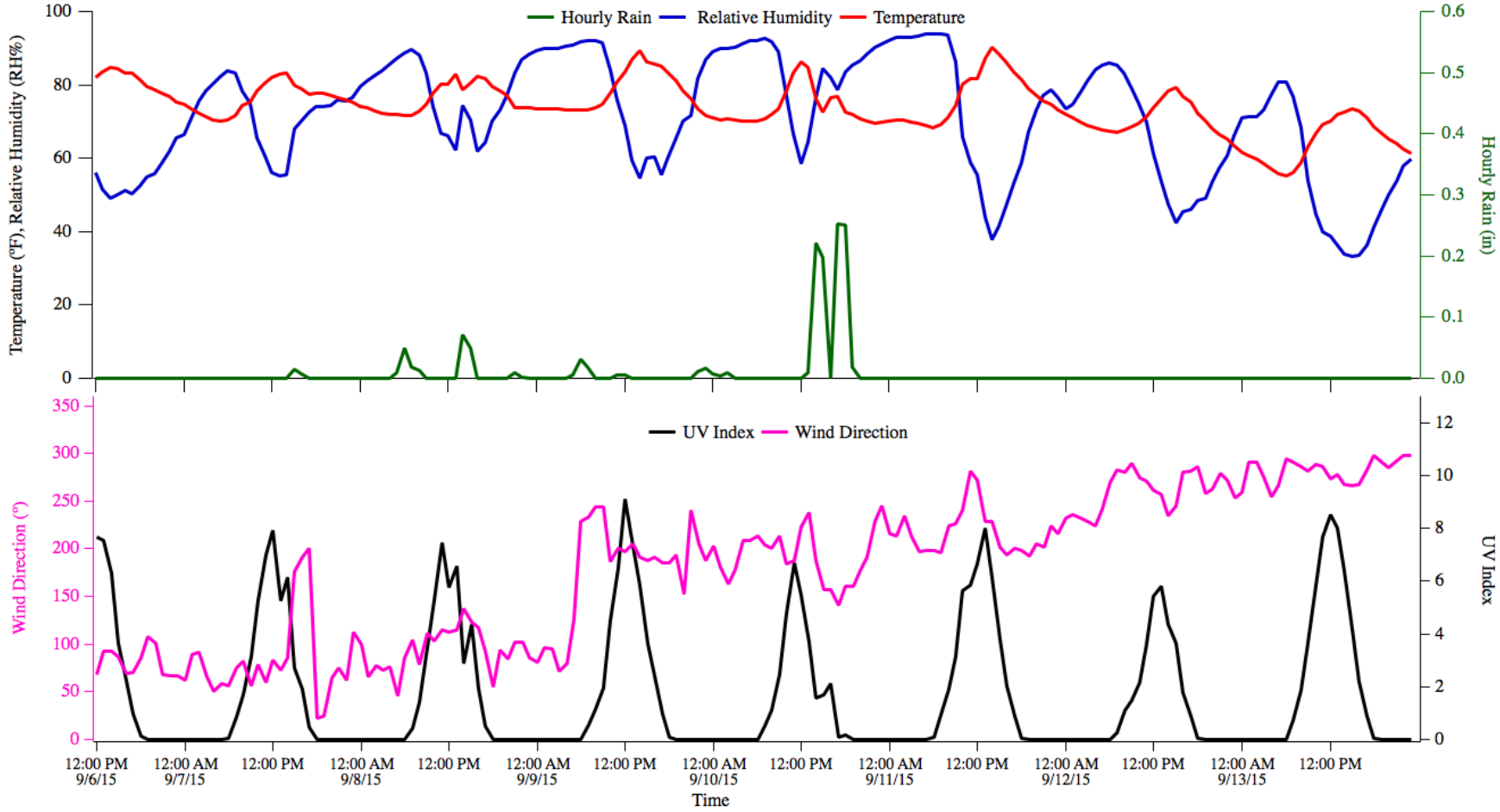

Figure 37: September meteorological data summary (hourly averages). Includes relative humidity, temperature, hourly rain, wind direction and UV index.

Sampling Site Pictures

Figure 38: ES&T rooftop sampling site pictures: a) rooftop view, b) Spincon II inside the doghouse during rainy days and c) Spincon II set up inside the doghouse.

REFERENCES

Augustin, S., S. Hartmann, B. Pummer, H. Grothe, D. Niedermeier, T. Clauss, J. Voigtländer, L. Tomsche, H. Wex and F. Stratmann (2012). "Immersion freezing of birch pollen washing water." Atmospheric Chemistry and Physics Discussions **12**(12): 32911-32943.

Bauer, H., M. Claeys, R. Vermeylen, E. Schueller, G. Weinke, A. Berger and H. Puxbaum (2008). "Arabitol and mannitol as tracers for the quantification of airborne fungal spores." Atmospheric Environment **42**(3): 588-593.

Bouvier, T., P. A. Del Giorgio and J. M. Gasol (2007). "A comparative study of the cytometric characteristics of high and low nucleic-acid bacterioplankton cells from different aquatic ecosystems." Environ Microbiol **9**(8): 2050-2066.

Bowers, R. M., S. McLetchie, R. Knight and N. Fierer (2011). "Spatial variability in airborne bacterial communities across land-use types and their relationship to the bacterial communities of potential source environments." ISME J **5**(4): 601-612.

Chen, P. S. and C. S. Li (2005). "Bioaerosol characterization by flow cytometry with fluorochrome." J Environ Monit **7**(10): 950-959.

Chi, M.-C. and C.-S. Li (2007). "Fluorochrome in Monitoring Atmospheric Bioaerosols and Correlations with Meteorological Factors and Air Pollutants." Aerosol Science and Technology **41**(7): 672-678.

DeLeon-Rodriguez, N., Terry L. Lathem, Luis M. Rodriguez-R, James M. Barazesh, Bruce E. Anderson, Andreas J. Beyersdorf, Luke D. Ziemba, Michael Bergin, Athanasios Nenes, and Konstantinos T. Konstantinidis. (2013). "Microbiome of the upper troposphere: Species composition and prevalence, effects of tropical storms, and atmospheric implications." Proceedings of the National Academy of Sciences **110**(7): 2575-2580.

Després, V. R., J. Alex Huffman, S. M. Burrows, C. Hoose, A. S. Safatov, G. Buryak, J. Fröhlich-Nowoisky, W. Elbert, M. O. Andreae, U. Pöschl and R. Jaenicke (2012). "Primary biological aerosol particles in the atmosphere: a review." Tellus B **64**(0).

Elbert, W., Taylor, P. E., Andreae, M. O., & Pöschl, U. (2007). "Contribution of fungi to primary biogenic aerosols in the atmosphere: wet and dry discharged spores, carbohydrates, and inorganic ions." Atmospheric Chemistry and Physics **7**(17): 4569-4588.

Gabey, A. M., M. W. Gallagher, J. Whitehead, J. R. Dorsey, P. H. Kaye and W. R. Stanley (2010). "Measurements and comparison of primary biological aerosol above and below a tropical forest canopy using a dual channel fluorescence spectrometer." Atmospheric Chemistry and Physics **10**(10): 4453-4466.

Gabey, A. M., W. R. Stanley, M. W. Gallagher and P. H. Kaye (2011). "The fluorescence properties of aerosol larger than 0.8 μm in urban and tropical rainforest locations." Atmospheric Chemistry and Physics **11**(11): 5491-5504.

Guindulain, T., J. Comas, and J. Vives-Rego (1997). "Use of nucleic acid dyes SYTO-13, TOTO-1, and YOYO-1 in the study of Escherichia coli and marine prokaryotic populations by flow cytometry." Applied and environmental microbiology **63**(11): 4608 - 4611.

Hernandez, M. P., A.; McCabe, K.; Kok, G.; Granger, G.; Baumgardner, D. (2016). "Composite Catalogues of Optical and Fluorescent Signatures Distinguish Bioaerosol Classes." Atmos. Meas. Tech. Discuss. **1**(17): 1867-8610.

Huffman, J. A., B. Treutlein, and U. Pöschl (2010). "Fluorescent biological aerosol particle concentrations and size distributions measured with an Ultraviolet Aerodynamic Particle Sizer (UV-APS) in Central Europe." Atmospheric Chemistry and Physics **10**(7): 3215-3233.

Huffman, J. A., A. J. Prenni, P. J. DeMott, C. Pöhlker, R. H. Mason, N. H. Robinson, J. Fröhlich-Nowoisky, Y. Tobo, V. R. Després, E. Garcia, D. J. Gochis, E. Harris, I. Müller-Germann, C. Ruzene, B. Schmer, B. Sinha, D. A. Day, M. O. Andreae, J. L. Jimenez, M. Gallagher, S. M. Kreidenweis, A. K. Bertram and U. Pöschl (2013). "High concentrations of biological aerosol particles and ice nuclei during and after rain." Atmospheric Chemistry and Physics **13**(13): 6151-6164.

Jaenicke, R. (2005). "Abundance of cellular material and proteins in the atmosphere." Science **308**(5718): 73-73.

Kesavan, J. and J. L. Sagripanti (2015). "Evaluation criteria for bioaerosol samplers." Environ Sci Process Impacts **17**(3): 638-645.

Lange, J. L. T., P S and Lynch, N (1997). "Application of flow cytometry and fluorescent in situ hybridization for assessment of exposures to airborne bacteria " Appl. Environ. Microbiol. **63**(4): 1557-1563.

.

Lebaron, P., P. Servais, H. Agogue, C. Courties and F. Joux (2001). "Does the high nucleic acid content of individual bacterial cells allow us to discriminate between active cells and inactive cells in aquatic systems?" Appl Environ Microbiol **67**(4): 1775-1782.

Li, D.-W., and Bryce Kendrick (1995). "A year-round study on functional relationships of airborne fungi with meteorological factors." International Journal of Biometeorology **39**(2): 74-80.

Liang, L., G. Engling, Y. Cheng, F. Duan, Z. Du and K. He (2013). "Rapid detection and quantification of fungal spores in the urban atmosphere by flow cytometry." Journal of Aerosol Science **66**: 179-186.

Möhler, O., DeMott, P. J., Vali, G., & Levin, Z. (2007). "Microbiology and atmospheric processes: the role of biological particles in cloud physics." Biogeosciences **4**(6): 1059-1071.

Morris, C. E., F. Conen, J. Alex Huffman, V. Phillips, U. Poschl and D. C. Sands (2014). "Bioprecipitation: a feedback cycle linking earth history, ecosystem dynamics and land use through biological ice nucleators in the atmosphere." Glob Chang Biol **20**(2): 341-351.

Muller, S. and G. Nebe-von-Caron (2010). "Functional single-cell analyses: flow cytometry and cell sorting of microbial populations and communities." FEMS Microbiol Rev **34**(4): 554-587.

Nir, R., Yisraeli, Y., Lamed, R., & Sahar, E. (1990). "Flow cytometry sorting of viable bacteria and yeasts according to beta-galactosidase activity." Applied and environmental microbiology **56**(12): 3861-3866.

Oliveira, M., H. Ribeiro, J. L. Delgado and I. Abreu (2009). "The effects of meteorological factors on airborne fungal spore concentration in two areas differing in urbanisation level." Int J Biometeorol **53**(1): 61-73.

Pöhlker, C., J. A. Huffman, J. D. Förster and U. Pöschl (2013). "Autofluorescence of atmospheric bioaerosols: spectral fingerprints and taxonomic trends of pollen." Atmospheric Measurement Techniques **6**(12): 3369-3392.

Pöhlker, C., J. A. Huffman and U. Pöschl (2012). "Autofluorescence of atmospheric bioaerosols: fluorescent biomolecules and potential interferences." Atmospheric Measurement Techniques **5**(1): 37-71.

Siljamo, P., M. Sofiev, E. Severova, H. Ranta, J. Kukkonen, S. Polevova, E. Kubin and A. Minin (2008). "Sources, impact and exchange of early-spring birch pollen in the Moscow region and Finland." Aerobiologia **24**(4): 211-230.

Taylor, P. E., K. W. Jacobson, J. M. House and M. M. Glovsky (2007). "Links between pollen, atopy and the asthma epidemic." Int Arch Allergy Immunol **144**(2): 162-170.

Toprak, E. and M. Schnaiter (2013). "Fluorescent biological aerosol particles measured with the Waveband Integrated Bioaerosol Sensor WIBS-4: laboratory tests combined with a one year field study." Atmospheric Chemistry and Physics **13**(1): 225-243.

Van Dilla, M. A., Langlois, R. G., Pinkel, D., Yajko, D., & Hadley, W. K. (1983). "Bacterial characterization by flow cytometry." Science **220**(4597): 620-622.

Wang, Y., F. Hammes, K. De Roy, W. Verstraete and N. Boon (2010). "Past, present and future applications of flow cytometry in aquatic microbiology." Trends Biotechnol **28**(8): 416-424.

Wu, Y.-H., C.-C. Chan, C. Y. Rao, C.-T. Lee, H.-H. Hsu, Y.-H. Chiu and H. J. Chao (2007). "Characteristics, determinants, and spatial variations of ambient fungal levels in the subtropical Taipei metropolis." Atmospheric Environment **41**(12): 2500-2509.